WIND-TUNNEL MODEL STUDY OF
SHOREHAM NUCLEAR POWER STATION
UNIT I LONG ISLAND LIGHTING COMPANY

by

R. N. Meroney

J. E. Cermak

and

F. H. Chaudhry

Progress Report

WIND-TUNNEL MODEL STUDY OF
SHOREHAM NUCLEAR POWER STATION
UNIT I LONG ISLAND LIGHTING COMPANY

by

R. N. Meroney

J. E. Cermak

and

F. H. Chaudhry

Prepared under contract to

Stone and Webster Engineering Corporation
Boston, Massachusetts

Fluid Dynamics and Diffusion Laboratory
College of Engineering
Colorado State University
Fort Collins, Colorado

July 1968   CER68-69RNM-JEC-FHC1

ABSTRACT

Tests were conducted in the Colorado State University 2 m square by 80 m long speed wind tunnel to determine the distribution of gas concentrations resulting from gaseous plumes released from short stacks on top of a model of the Shoreham Nuclear Power Station reactor building. Basic tests were made on the reactor building model in an adiabatic atmosphere having a logarithmic upstream velocity profile. The effects of absolute wind velocity, and approach azimuth, and variable stack velocities were examined. Data obtained included photographs of model smoke plume tracjectories, photographs of plume ground impingement shown by indicator points, and local concentrations of Kr-85 at downstream locations.

TABLE OF CONTENTS

Chapter		Page

LIST OF FIGURES

iv

LIST OF SYMBOLS

Symbol		Definition
A	=	Area of the projection of the reactor building on a plane transverse to the upstream flow direction = DH
C	=	Entrainment parameter
c	=	Local concentration
D	=	Reactor building diameter
H	=	Reactor building height
h	=	Stack height
K	=	Experimentally determined distribution function = $CAV/\overset{o}{Q}$
L	=	Reference length
$\overset{o}{Q}$	=	Gas source release rate
R_e	=	Reynold's number = scaling parameter relating ratio of viscous and inertial forces in a flow system = $\dfrac{VL}{\nu}$
R_1 or R_2	=	Critical velocity ratios at 300 m and 150 m = $\dfrac{V_s}{V}$
V_∞	=	Maximum mean velocity above tunnel boundary layer
V	=	Mean wind velocity at some reference height
V_s	=	Velocity of effluent at stack exit
X_c	=	Downstream extent of separation cavity region
x,y,z	=	General coordinates; downwind, lateral, upward
Z_o	=	Surface roughness parameter
θ	=	Azimuth angle of upwind direction measured from magnetic north
ν	=	Kinematic viscosity of atmosphere

I. INTRODUCTION

Commercial nuclear power reactors are generally enclosed in an airtight shell which prevents arbitrary release of gases or air to the atmosphere. In addition, the reactors are designed and operated with strict controls for the disposal of waste gases. During normal operation, radioactive isotopes of such gases as xenon and krypton, produced as a result of the fission process, are contained within the fuel rods. For long-term operation of the plant, design provisions are usually made for safely accommodating a slight leakage of gases from a small percentage of the fuel rods which comprise the reactor core. For some boiling water reactors, such as the Shoreham Nuclear Power Station, a holdup system will be employed for retention of the gases for radioactive decay and until such a time that meteorological conditions are favorable for dilution and dispersion. Under certain hypothetical conditions, it may be necessary to make a release in meteorologically unfavorable situations. Hence, it is necessary to design gas exhaust systems such that adequate dispersal of gaseous materials will occur under any plausible condition.

It has been a traditional design technique to release the various gases through the top of a tall stack located near the containment vessel, where the stack is at least two and one-half times taller than nearby buildings. Calculation of peak and mean ground concentrations of these gases are then based on some semi-empirical model which relates the release rate from an elevated point source to the concentration at some point downwind. Models have been suggested by Sutton, Hay and Pasquill, Roberts and Cramer.[1,2,3,4] These models require the assumptions of plane homogeneous atmospheric turbulence and constant mean lateral and mean vertical velocities. These assumptions are satisfied for a point release over a flat undisturbed terrain.

In addition, considerable effort has been made to determine the effects of vertical stack velocity and gas buoyancy on the effective

stack release height. Recently Carson and Moses[5] have reviewed over 15 plume rise formulas available to calculate effective stack heights for conditions where there are no effects from local terrain or buildings. They concluded that no available plume rise equation can be expected to accurately predict short term plume rise.

Often it is desirable due to aesthetic, cost, and public relation reasons to utilize a shorter stack or vent connected directly to the reactor building. In these cases plume dispersion is sufficiently modified by the presence of the local building structure or ground topography that the only approach available is one of wind tunnel model tests. [6,7]

A number of wind tunnel studies have considered the effects of variations in a single building geometry on plume entrainment and dispersion. [8,9,10,11] These studies have permitted the specification of pertinent scaling criteria for model studies of plume excursions near buildings. Model laws will be discussed in greater detail in Section II.

Since each arrangement of reactor building and auxiliary buildings or terrain may have separate effects on the generation of mechanical turbulence and mean flow movement, any specific gas dispersion problem will require individual tests. Hence there exist in the literature descriptions of a variety of different model studies on reactor and industrial plants. [7,12,13,14,15,16] These studies are significant in that their results have been essentially confirmed by either direct prototype measurements or the absence of the gases or dusts the study was directed to remove. References 12), 13), 15), and 16) incorporate such comparisons within their text. Reference 7) has recently been compared with prototype measurements at the National Reactor Testing Station in

Southeast Idaho. [17] Agreement of the diffusion concentration results were very satisfactory. Martin favorably compared his wind tunnel study measurements about a model of the Ford Nuclear Reactor at the University of Michigan with prototype measurements. [16] Finally, Munn and Cole have taken diffusion measurements on a power station complex at the National Research Council, Ottawa, Canada, to confirm the general entrainment criteria suggested by the model studies of Davies and Moore. [13, 18]

It is the purpose of this study to investigate the effect of the Shoreham Nuclear Power Station complex on effluent releases from a short stack on the roof of the reactor building, to determine the wind direction configuration for maximum entrainment, and to determine the feasibility of increasing stack velocity and flow rate to elevate the plume to a level where entrainment into the building separation cavities and subsequent dispersion at ground level is absent.

In Section II the modeling criteria necessary to simulate atmospheric motions over such a site are listed. Section III describes the experimental equipment. Finally, Sections IV, and V discuss the results obtained and their significance.

II. SIMULATION OF ATMOSPHERIC MOTIONS

The use of wind tunnel for model tests of atmospheric gas diffusion is dependent on the expression of concentration results in a non-dimensional coefficient whose value is independent of the variations in scale between model and prototype. The concentration coefficients will only be independent of scale if certain similarity criteria are met by the modeled flows. These criteria are generally understood as a result of analysis of experience, and they are discussed in detail in References 8, 16, and 19. Basically, these model laws may be divided into those of geometric, dynamic, and kinematic similarity. In addition, one must specify upstream and ground boundary conditions.

For the present case of the Shoreham Reactor site, geometric similarity is satisfied by an undistorted model of size ratio 1:200. This scale ratio was chosen to optimize measuring scale and minimize wind tunnel blockage[*]. In addition, this scale ratio allowed the wind tunnel boundary layer to extend a distance above the model complex.

Dynamic similarity is dependent upon equivalence of the inertial to buoyancy force ratio from model to prototype. Normally, this is assumed by equivalence of the atmospheric Froude Number (Richardson number) and the control of stack gas densities; however, since only the neutral stratification problem was to be modeled and since the radioactive

---

[*] A consideration in the selection of model scale is the degree of blockage presented by the model. The ratio of projected model area to area of the wind tunnel cross-section should not exceed 1 to 2%. A scale of 1:200 for the Shoreham facility produces a blockage ratio of 1.8%.

effluent may be assumed at ambient temperatures due to dilution before
release, no special precautions were necessary for the modeled flow.
Non-buoyant stack gases and a neutral stratification were utilized.

Kinematic similarity requires the scaled equivalence of stream-
line movement of the air over prototype and model. It has been shown by
Golden [7] that flow around geometrically similar sharp-edged buildings at
ambient temperatures in a neutrally stratified atmosphere should be dy-
namically similar when the approaching flow is dynamically similar. This
approach depends upon producing flows in which the flow characteristics
become constant (independent of Reynolds Number) if a lower limit of the
Reynolds number is exceeded. For example, the resistance coefficient for
flow in a sufficiently rough pipe as shown in Schlichting (20, p 521) is
constant for a Reynolds number larger than $2x10^4$. This implies that
surface or drag forces are directly proportional to the mean flow speed
squared. In turn, this condition is the necessary condition for mean
turbulence statistics such as root-mean square value and correlation
coefficient of the turbulence velocity components to be equal for the
model and the prototype flow. [8,19]

Golden, as cited by Halitsky [7,8], found that for flow about a
cube for Reynolds numbers above 11,000, there was no change in concen-
tration measurements. The minimum Reynolds number encountered in the
present study was 13,000 based on the Reactor model width of 0.207 m and
a minimum velocity of 1 mps. Correlation tests of flow about the Rock
of Gibralter, flow over Pt. Arguello, California, and flow over San
Nicolas Island, California, may be cited as examples of large Reynolds
number flows which have been modeled successfully in a wind
tunnel. [21,22,23]

Buildings and building complexes produce nonuniform fields of flow which perturb the regular upstream atmospheric wind profiles. Around each building a boundary layer exists, where the velocity is zero at the surface but increases rapidly to a relatively constant valve or short distance from the building wall. Outside of the boundary layer and downstream there exists a region of low velocities and pressures called the cavity. In this region circulations are such that flow may actually reverse with respect to the upstream winds. Surrounding the cavity but extending further downstream is a parabolic region called the wake in which the presence of the building is still evident in terms of deviations of velocity, turbulence, and pressure from conditions found in the up-stream atmospheric boundary layer, (See Figure 3a).

The formation of the wake and cavity regions are associated with a phenomena called boundary layer separation. Under certain conditions the boundary layer actually detaches and enters the flow streaming about the building. This may occur at the corner of a sharp edged building or on a curved surface if the pressure increases due to a decelerating flow field. The separated boundary layer forms a sheet which completely surrounds the cavity region which contains relatively stagnant fluid. The extent of the cavity region for the Shoreham Power Station reactor building may be approximated by

$$X_c = 5 \text{ or } 6 \sqrt{\frac{A}{\pi}} = 140 \text{ to } 170 \text{ meters.} [8]$$

On buildings with rounded surfaces, such as the Shoreham reactor containment vessel, the flow is such that the separation point is dependent upon the Reynolds number. If the boundary flow is laminar then separation will occur approximately 80 to 90° from the stagnation point, while if the flow is turbulent separation will be delayed until

110 to 120° from the stagnation point. Variation in the separation point will introduce changes into the remainder of the flow field. For the turbulent boundary layer case pressures behind the cylinder will be nearly ambient.

It is generally expected for large curved surfaces in the atmospheric boundary that turbulent separation occurs, especially when there are other upstream structures to perturb the flow.[8] It was expected that the modeled reactor vessel in the wind tunnel flow would also exhibit turbulent separation. This would result from the presence of the upstream building complex, the logarithmic upstream velocity profile, and the sharp edged geometry of the top region of the containment structure.

The turbulent separation condition has been confirmed in two ways. First a cylinder of similar scale to the model reactor was attached to a strain gauge shear plate and studied in the wind tunnel over the complete range of velocities available. The drag force measurements produced a constant drag coefficient for the entire velocity range. (See Figure 3b). The absence of a drop in drag coefficient indicates that the flow field did not pass through a transition resulting from a move in the separation position. In addition, pressure taps on the actual model of the Shoreham reactor structure were monitored around the circumference of the building at six heights. In those regions near the top of the building most subject to Reynolds number effects the separation is not evident until 120°. (See Figure 4).

The interaction of the emitted effluent with the wind is governed by the ratio of their respective momenta.[7,8,9,13,16] When the prototype and model plumes have the same density this reduces to a ratio of velocities. In this study the stack areas were geometrically scaled and

the velocities studied were 15 and 61 meters per second. The wind velocity was adjusted in a range from 1 to 35 meters per second.

Finally, the need for scaling of the atmospheric mean wind profile is demonstrated in Reference 11. Substitutions of a uniform velocity profile for a logarithmic profile results in three fold variation in the dimensionless pressure coefficient downstream of a model building.

Such variance in the pressure fields indicates a strong effect of the upstream wind profile on the kinematic behavior of the fluid near the building comples. The only tunnel currently capable of generating a turbulent boundary layer thick enough for a 1:200 model scale is the Meteorological Wind Tunnel at Colorado State University. Other investigators have attempted to generate logarithmic profiles in short tunnels by inserting special grids upstream of the test secion; however, this technique normally creates a nontypical turbulence field which decays rapidly downstream.

The length scale used for scaling the velocity profile is the roughness height Z_o. [19] For the Shoreham Nuclear reactor site typical roughness lengths for land to sea breezes is one meter, while sea to land winds are typified by a length of 1 cm. [24] This means the critical sea to land wind velocities could be modeled in the wind tunnel by a roughness scale of 1/200 cm, as essentially a smooth upstream surface. A turbulent boundary layer approximately 0.5 m thick was produced by an upstream fetch of 15 m in the wind tunnel.

III. TEST APPARATUS

A. Wind Tunnel

Tests were conducted on the Army Meteorological Wind Tunnel in the Fluid Dynamics and Diffusion Laboratory at Colorado State University. The tunnel, specifically designed to study fluid phenomena of the atmosphere, has a 2 meter square by 26 meter long test section with an adjustable ceiling to provide a zero pressure gradient over modeled terrain,[25] (See Figure 1). A trip fence, located just upstream from the test section serves to stabilize the flow pattern as well as provide a thicker turbulent boundary layer. Mean velocities may be adjusted between 0 to 37 mps, and boundary layers 0.5 m thick may be obtained.

B. Model

The model consisted of the reactor shell, the stack, and the auxiliary buildings constructed to a linear scale of 1:200. The basic flat topography was reproduced by maintaining the model complex on a large circular plywood sheet which could be rotated into various wind attack angles. The surface roughness was typically 1 cm for the prototype and could be satisfactorily modeled by the smooth tunnel floor. Figure 2 shows two views of the model in the tunnel.

The model was built to dimensions taken from a Stone and Webster Drawing 11600-FM-S106A, dated 10-27-67. A set of static pressure taps were incorporated in the Lucite plastic walls of the containment vessel. Model stacks were inserted into a threaded hole in the center of the vessel roof. Two model stacks were studied; one equivalent to a 3.0 meter tall prototype stack with an exit area of 0.031 sq meters, and a

second equivalent to 3.0 meter tall prototype stack with an exit area of 0.465 sq meters. Auxiliary buildings were constructed from styrofoam and painted with a latex paint.

A single tall stack was also constructed for comparison of plume behavior to that over the reactor complex. The stack had a height equivalent to the release height of the stack on the containment vessel roof and the same two exit areas.

C. Wind Profiles, Pressure, and Drag Measurement

A pitot-static tube was used to measure upstream velocity profiles and set mean tunnel speeds. Pitot-static tube output was analyzed by a Transonic Model A, Type 120 electronic pressure meter. This instrument also monitored the static pressure taps on the model side wall.

Drag measurements were made by means of a shear plate, 0.6 m x 0.6 m in area, inserted in the wind tunnel floor. The shear plate is instrumented with strain gauges and can measure drag forces as small as 0.001 to 0.0001 grams.[26] A right circular cylinder having the same size as the model reactor buildings was mounted on the shear plates. Measurements provided the variation of drag coefficient with Reynolds number.

D. Visualization Techniques

Smoke was used to define plume behavior over the reactor complex. The smoke was produced by bubbling compressed air through a container of titanium-tetrachloride located outside the wind tunnel and transported through the tunnel wall by means of a tygon tube terminating at the stack inlet within the model containment vessel. A visible record was obtained by means of pictures taken with (a) a series 100 Polaroid camera with integrating shutter and (b) a Speed-graphic camera utilizing

4 x 5 in. Tri-X film. (The Speed-graphic camera operated at an f-stop of 4.5 with a shutter speed of 1/25 second.)

Plume contact with the ground surface was determined by an indicator point method. The indicator point was applied to the ground surface of the model, and it consisted of white water-base latex paint mixed with "congo-red" (sodium tetrazodiphenylnapthionate - an organic indicator of pH intensity). Diluted hydrochloric acid was applied to the painted surface which sensitized the surface to the presence of anhydrous ammonia. Anhydrous ammonia was then released at the appropriate rate from the reactor stack into the air stream. A trace of the diffusion plume of ammonia, indicating the surface wind contact, showed as a pink area on the blue background of the model. These areas were also recorded photographically.

E. Gas Tracer Technique[*]

After the flow in the tunnel was stabilized, a mixture of Kr-85 and air was released from the model reactor stack, and samples of air were withdrawn from the tunnel and analyzed. The flow rate of Kr-85 mixture was controlled by a pressure regulator at the bottle outlet and monitored by a Fisher and Porter flowmeter. Source concentration was 0.169 μ-curie /cc of Kr-85, a beta emitter (half life - 10.3 years).

A sampling rake of eight probes was manufactured from 2 mm diameter hypodermic tubing and was mounted on a traversing carriage whose horizontal and vertical position was controlled remotely from outside the tunnel. Concentrations were measured at gound levels at equivalent

---

[*] This apparatus was developed under the Public Health Service, Contract No. DHEW, 5R01 AP00091-07.

scaled distances of 150 and 300 m downwind and at vertical elevations of 31 m and 62 m at the 300 m downwind distance. Samples were aspirated at a constant rate of 500 cc/min into eight TGC-308 Tracerlab Geiger Mueller side wall cylindrical counters. Samples were flushed through the counting tubes for at least two minutes, valve A in Figure 5b was closed, and each sample was subsequently counted for one minute on a Nuclear Chicago Ultra-scaler Model 192A. All samples counted were ad-justed for background radiation (See Figures 5a and 5b).

IV. TEST PROGRAM AND RESULTS

A. Test Program

The test program consisted of (1) a qualitative study of the flow field around the reactor by visual observation of the smoke plume trajectory released on the reactor roof; (2) a qualitative examination of the extent of plume ground contact as displayed by indicator paint color changes, and (3) a quantitative study of gas concentrations produced by the release of Kr-85 from the roof stack. The test conditions are summarized in Tables 1 and 2. The test program was accomplished in two parts: Phase A involved a stack gas release velocity of 15.2 m/sec and Phase B utilized a stack gas release velocity of 60.8 m/sec.

Angular locations of the approach winds are referred to in terms of azimuth angles from magnetic north. Downwind distances refer to lengths as measured from the center of the reactor containment vessel. Unless otherwise noted, the term wind velocity refers to the velocity in the free stream above the tunnel boundary layer; however, a velocity at any reference height is available by referring to the velocity profiles (Figure 6).

TABLE 1. EFFLUX CONDITIONS STUDIED

Program Phase	Prototype			Model	
	Stack Area (m^2)	Efflux Rate (m^3/min)	Jet Velocity (m/sec)	Stack Diameter (cm)	Jet Velocity (m/sec)
A	0.465	425.0	15.2	0.394	15.2
	0.031	28.3	15.2	0.100	15.2
B	0.465	1700.0	60.8	0.394	60.8

TABLE 2. SUMMARY OF DATA COLLECTION PROGRAM

Phase A:

Wind Direction (Azimuth)	Wind Velocity (m/sec)	Stack Diameter (cm)	Jet Velocity (m/sec)	Photos of Smoke	Surface Visualization	Concentration Profiles
0°	(1,2,4,6, 8,10,15)	0.394	15.2	yes	yes	no
30°				yes	yes	no
90°				yes	yes	no
180°				yes	yes	no
315°				no	yes	no
330°		0.394		yes	yes	yes
330°		0.100		no	yes	yes
345°		0.394		no	yes	no

Phase B:

Wind Direction (Azimuth)	Wind Velocity (m/sec)	Stack Diameter (cm)	Jet Velocity (m/sec)	Photos of Smoke	Surface Visualization	Concentration Profiles
0°	(4,8,10,15 20,25,30, 35)	0.394	60.8	yes	yes	no
315°				yes	yes	no
330°				yes	yes	yes

Single Stack:

Wind Direction (Azimuth)	Wind Velocity (m/sec)	Stack Diameter (cm)	Jet Velocity (m/sec)	Photos of Smoke	Surface Visualization	Concentration Profiles
0°	(1,2,4,6, 8,10,15)	0.394	15.2	yes	yes	no
0°	(4,8,10, 15,20, 25,30)		60.8	yes	yes	no

B. Test Results: Visualization

The test results consist of photographs and sketches showing the general nature of air flow and diffusion in the vicinity of the model reactor, (Figure 7 to Figure 15). A general understanding of wake and cavity flows is necessary for an interpretation of the plume behavior - see Reference 8.

The sequence of photographs shown in Figure 7 shows side views of the behavior of a smoke plume released at various free stream velocities. At low wind speeds the plume breaks through the streamline separating the cavity and the displaced flows above the complex. Subsequently the gas behaves as a plume released at an elevated point and is convected downstream. As the wind speed increases the stack effluent plume is bent over and behaves as though it were released at increasingly lower effective heights. At a sufficiently large free stream velocity the plume intermittently fails to penetrate the building cavity streamline, and gas is brought to the ground at points near the building. At even higher wind speeds the plume becomes completely entrained in the building cavity. Entrainment, as utilized herein, will be understood as the presence of any of the gas released from the roof exhaust stack in the reactor building separation cavity. A small amount of entrainment usually first occurs under conditions where the gas plume follows the cavity separation stream line to the downstream cavity stagnation point from which it diffuses upstream into the cavity proper. Downwash will be understood as severe entrainment where the plume does not penetrate the separation stream-line but rather ventilates directly into the cavity region. Figures 8 to 11 display the outlines of the visual smoke plume for various wind speeds and wind approach angles for Phase A of the program.

For most wind approach angles ($0°$ to $300°$) the building complex appears to have a similar effect on plume entrainment. Davies and Moore suggested quantitative criteria for the tendency of a building to draw a gaseous plume released from a roof stack into the separation cavity. [13] They suggested the specification of the ratios, R_1 and R_2, of stack velocity to reference wind speed at which continuous plume contact becomes evident at distances of 300 m and 150 m downstream from the source position. The critical velocity ratio R_2 of efflux velocity to wind velocity at which the turbulent motions in the wake region were great enough to disrupt the plume and produce contact at an equivalent distance of 150 m downstream was between 2 and 4. In addition, for the $180°$ reactor complex configuration, the smoke was strongly entrained behind the large turbine building over its entire length at a R_2 ratio of 4.

Between $315°$ and $345°$ an aggravated case of plume entrainment occurred. Plume dispersion into the building cavity was evident at R_2 ratios of 7 to 15. Separate releases of smoke on the upstream edges of the turbine building indicated a vortex development from the turbine roof corners which is drawn downward between the reactor containment vessel and the turbine plant. This resulted in an extreme low pressure region with very strong downwash. The strong low pressure region was also evident in the polar static pressure profile about the reactor vessel, (Figure 4).

The impingement indicating paint confirmed the results of the smoke visualization. Figure 12 indicates the typical contact parabola of the plume, while Figure 13 displays the adverse entrainment downwind of the turbine building for an azimuth angle of $180°$. Table 3 summarizes the minimum contact distances for various wind speeds and approach azimuth angles.

In Phase B a higher effluent velocity and flow rate were utilized to determine if the effects of downwash on the effluent dispersion could be avoided. Figures 14 and 15 display the smoke plume outline for an efflux velocity of 60.8 mps at various wind speeds and azimuth angles. The critical configuration of the reactor complex remained between 315° to 345°; however, the value of the ratio R_2 appeard to improve.

Table 3 also summarizes the equivalent distances to plume contact for a stack velocity of 60.8 m/sec. The effect on the impingement indicating paint was harder to interpret at higher free stream velocities; however, strong downwash into the low pressure regime between the containment vessel and turbine building was found. Paint applied to the side walls of the model containment vessel indicated rotation of the plume down the reactor vessel walls into the low pressure region when the free wind speed exceeded a minimum entrainment condition.

Table 4 tabulates the values of the ratios R_1 and R_2 versus wind azimuth angles and stack efflux velocities. R_1 and R_2 are respectively the ratio of stack velocity to reference wind speed at which continuous plume contact becomes evident at equivalent downstream distances of 300 m and 150 m. [13]

Smoke and ammonia were also released from a single stack (Figure 20) for effluent velocities of 15.2 and 60.8 mps. No evidence of ground contact was found over the entire range of wind speeds. The smoke plume could not be observed to contact the gound at equivalent prototype distances less than 600 meters downstream. Further definition was difficult due to cloud dispersion.

C. Test Results: Concentration Measurements

Since the conventional point-source diffusion equations cannot be used for predicting diffusion near objects which cause the wind to be nonuniform and nonhomogeneous in velocity and turbulence, it is necessary to calculate gaseous concentrations on the basis of experimental data. It is convenient to report dilution results in terms of a nondimensional factor independent of model to prototype scale.

In References 8 and 16 the problem of similarity for diffusing plumes is discussed in detail. It is suggested that concentration measurements be transformed to K-isopleths by the formula

$$K = \frac{c}{\overset{\circ}{Q}/AV}$$

where   c = sample volume concentration

A = frontally projected area of reactor containment vessel

V = mean wind velocity at some reference height

$\overset{\circ}{Q}$ = gas source release rate.

Concentration measurements were made at ground level at equivalent distances of 150 m and 300 m downstream from the model reactor vessel and at vertical heights of 31 m and 62 m at the 300 m position. Samples were taken at eight lateral positions normal to the mean wind direction. Table 5 summarizes the values of the concentration measurements. The value of K at each sample point was calculated according to the formula above - a reference wind speed was selected from the profiles of vertical velocity at an equivalent position of 10 m (Figure 6). The point values were then plotted on graphs corresponding to a surveyed plane.

Figures 16 and 17 display the results of Phase A measurements for the critical configuration angle. Figure 18 summarizes the results of

Phase B for the same angle. It should be pointed out that the K field will be a function of $\frac{V_s}{U_\infty}$ and a new flow configuration should be established for each value of $\frac{V_s}{U_\infty}$ (See Figure 19).

When interpreting model diffusion measurements it is important to remember that there can be considerable difference between the instantaneous concentration in a plume and the average concentration due to horizontal meandering. The average dilution factors near a building complex will correlate well with wind tunnel dilution factors since the mechanical turbulence of the wake and cavity region dominate the dispersion. In the wind tunnel a plume does not generally meander due to the absence of large scale eddies. Thus it is found that field measurements of peak concentrations, which effectively eliminate horizontal meandering, should correlate with the wind tunnel data. [16] In order to compare downwind measurements of dispersion to predict average field concentrations it is necessary to use data on peak-to-mean concentration ratio as gathered by Singer, et al. Their data is correlated in terms of the gustiness categories suggested by Pasquill for a variety of terrain conditions. [27] It is possible to determine the frequency of different gustiness categories for a specific site. [28] Direct use of wind tunnel data at points removed from the building cavity region may underestimate the dilution capacity of a site by a factor of 4 unless these adjustments are considered. [16]

V. CONCLUSIONS AND RECOMMENDATIONS

This research was undertaken to determine by a wind tunnel model study the dispersion of radioactive gases released from a short stack on top of the reactor containment building in the Shoreham Nuclear Power Station, to determine if a wind approach angle existed which resulted in aggravated entrainment, and to determine if the effects of downwash could be alleviated with high effluent flow rates and vertical stack velocities.

On the basis of the experimental measurements reported herein, the following comments may be made:

1. Drag and static pressure measurements support the assumption that the scale model of the Shoreham Nuclear Power Station should satisfactorily simulate prototype conditions in the vicinity of the site.

2. At low efflux stack velocities entrainment will occur at efflux ratios of R_1 and R_2 , respectively, of 4 and 8 for most wind azimuths from 0° to 270°.

3. At low efflux stack velocities entrainment is aggravated by the local building geometries such that between wind azimuths of 270° to 360° efflux ratios R_1 and R_2 exceed 7.

4. A somewhat less critical aggravated entrainment also occurs at an azimuth of 180° where R_1 and R_2 equal 5.4 and 10 respectively

5. Higher efflux stack velocities reduce the tendency toward entrainment. At 0° R_1 and R_2 average 4.2 and 7.4 respectively. Between 270° to 360° R_1 and R_2 average 4.2 and 7.4.

6. Estimates of gaseous concentration may be made from the K-profiles reported in Figures 16, 17, and 18. Examples of calculations for full scale applications may be found in Chapter 5 of Reference 16.

The measurements reported in this study are of a preliminary nature; however, it is evident that higher effluent rates from the reactor stack reduced the entrainment. Hence it is recommended that further model tests be made to determine the effects in plume dispersion of local terrain, of variations in stack height or location, and of possible changes in the nuclear complex building geometry or architecture.

REFERENCES

1.   Sutton, O. G., "The Theoretical Distribution of Airborne Pollution
         from Factory Chimneys," Quar. J. R. Meteor. Soc. 73,
         p. 426 (1947).

2.   Pasquill, F., Atmospheric Diffusion, D. Van Nostrand Co.,
         London (1962).

3.   Roberts, O.F.T., "The Theoretical Scaling of Smoke in a Turbulent
         Atmosphere," Proc. Roy. Soc., A. 104, p. 640.

4.   Cramer, H. E., "A Practical Method for Estimating the Dispersal
         of Atmospheric Contaminants," Proceedings, First Nat'l
         Conf. on Appl. Meteor, Amer. Meteor Soc., C. pp. 33-35.
         Hartford, Conn., (Oct. 1957).

5.   Carson, J. E., and H. Moses, "Validity of Currently Popular Plume
         Rise Formulas," USAEC Meteorological Information Meeting,
         (September 11-14, 1967), Chalk River, Canada, AECL-2787,
         pp. 1-15.

6.   Moses, H; G. H. Strom; and J. E. Carson, "Effects of Meteoro-
         logical and Engineering Factors on Stack Plume Rise,"
         Nuclear Safety, Vol. 6, # 1, (Fall 1964), pp. 1-19.

7.   Halitsky, J.; J. Golden; P. Halpern; and P. Wu, "Wind Tunnel
         Tests of Gas Diffusion from a Leak in the Shell of a
         Nuclear Power Reactor and from a Nearby Stack,"
         Geophysical Sciences Laboratory Report No. 63-2,
         New York University, (April 1963).

8.   Halitsky, J., "Gas Diffusion Near Buildings," Geophysical
         Science Laboratory Report No. 63-3, New York University,
         (February 1963).

9.   Strom, G. H.; M. Hackman, and E. J. Kaplin, "Atmospheric Dispersal
         of Industrial Stack Gases Determined by Concentration
         Measurements in Scale Model Wind Tunnel Experiments,"
         J. of APCA, Vol. 7, # 3, pp. 198-204, (November 1957).

10.   Evans, B. H., "Natural Air Flow Around Buildings," Research
         Report 59, Texas. Engineering Experiment Station, (1957).

11.   Jensen, M., and N. Frank, "Model-Scale Test in Turbulent Wind,
         Part I," The Danish Technical Press, Copenhagen, (1963).

12.   Kalinske, A. A., "Wind Tunnel Studies of Gas Diffusion in a
         Typical Japanese Urban District," National Defense Res.
         Council OSCRD Informal Report # 10.3A-48 and 48a, (1945).

13. Davies, P.O.A.L., and P. J. Moore, "Experiments on the Behavior of Effluent Emitted from Stacks at or Near the Roof Level of Tall Reactor Buildings," Int. Jour. Air Water Pollution. Vol. 8, pp. 515-533, (1964).

14. Sherlock, R. H., and E. A. Stalker, "The Control of Gases in the Wake of Smokestacks," Mechanical Engineering Vol. 62, # 6, pp. 455-458, (June 1940).

15. Hohenleiten, H. L. von and E. Wolf, "Wind Tunnel Tests to Establish Stack Heights for the Riverside Generating Station," Trans ASME Vol. 64, pp. 671-683, (Oct. 1942).

16. Martin, J. E., "The Correlation of Wind Tunnel and Field Measurements of Gas Diffusion Using Kr-85 as a Tracer," Ph.D. Thesis, MMPP 272, University of Michigan, (June 1965).

17. Dickson, G. E. Start and E. H. Markee, Jr., "Airodynamic Effects of the EBR-II Containment Vessel Complex on Effluent Concentrations," USAEC Meteorological Information Meeting, Chalk River, Canada, AECL-2787, pp. 87-104, (September 11-14, 1967).

18. Munn, R. E., and A. F. W. Cole, "Turbulence and Diffusion in the Wake of a Building," Atmospheric Environment, Vol. 1, pp. 33-43, (1967).

19. Cermak, J. E., et al., "Simulation of Atmospheric Motion by Wind-Tunnel Flows," Colorado State University, Report Number CER66-JEC-VAS-EJP-GJB-HC-RNM-SI-17, (May 1966).

20. Schlichting, H., Boundary Layer Theory, McGraw Hill, New York, (1960).

21. Field, J. H., and R. Warden, "A Survey of the Air Currents in the Bay of Gibraltar, 1929-1930," Air Ministry, Geophys, Mem. No. 59, London (1933).

22. Cermak, J. E., and J. Peterka, "Simulation of Wind Fields Over Point Arguello, California, by Wind-Tunnel Flow Over a Topographical Model," Final Report, U. S. Navy Contract N 126(61756)34361 A(PMR), Colorado State University Report Number CER65JEC-JAP64, (December 1965).

23. Meroney, R. N., and J. E. Cermak, "Wind Tunnel Modeling of Flow and Diffusion Over San Nicolas Island, California," U. S. Navy Contract N123(61756)50192A(PMR), Colorado State University Report Number CER66-67RNM-JEC44, (September 1967).

24. Koehler, S. B., Stone and Webster Engineering Corporation, Boston, Mass., Private Communication (June 1968).

25. Plate, E. J., and J. E. Cermak, "Micro-Meteorological Wind-Tunnel Facility: Description and Characteristics," Fluid Dynamics and Diffusion Laboratory Report Number CER63EJP-JEC9, Colorado State University (1963).

26. Integrated Army Meteorological Wind-Tunnel Research Program, Eleventh Quarterly Progress Report, (1 November 1967 - 31 January 1968), 22 pages.

27. Singer, I. A., and I. Kazukiko, and G. D. Roman, "Peak to Mean Pollutant Concentration Ratios for Various Terrain and Vegetative Cover," Journal APCA, Vol. 13, # 1, p. 40, (1963).

28. Singer, I. A., and M. E. Smith, "The Relation of Gustiness to Other Meteorological Parameters," Jour. Meteor. Vol. 10, # 2, (1953).

29. Barry, P. J., "Estimation of Downwind Concentration of Airborne Effluents Discharged in the Neighborhood of Buildings," Atomic Energy of Canada, Limited, Report AECL-2043, (July 1964).

TABLE 3   MINIMUM DISTANCES TO PLUME CONTACT IN METERS

$$V_s = 15.2 \text{ mps}$$

V_∞ \ θ	180°	30°	0°	-15°	-30°	-45°
1 mps	400	none	none	250	100	120
2	240	400	none	240	60	50
4	*	120	300	150	45	45
6	*	105	275	60	*	*
8	*	90	150	*	*	*
10	*	60	60	*	*	*
15	*	*	*	*	*	*

$$V_s = 60.8 \text{ mps}$$

V_∞ \ θ	0°	-30°
4	none	none
8	350	350
15	150	150
20	*	*
25	*	*

* Complete contact downstream of the structure.

TABLE 4   EFFLUX TO WIND SPEED RATIOS
FOR VARIOUS AZIMUTH ANGLES
AND STACK EFFLUX VELOCITIES

V_s = 15.2 mps

θ	R	R_1	R_2
180°		10	5.4
30°		8.1	4.0
0°		4.0	2.1
-15°		<16	4.0
-30°		<16	<16
-45°		<16	<16

V_s = 60.8 mps

θ	R	R_1	R_2
0°		7.4	4.2
-30°		7.4	4.2

TABLE 5

CONCENTRATION DOWNSTREAM OF REACTOR BUILDING
(micro, micro curies per cubic centimeter)

Concentration Data

v_s = 15.2 mps

θ = -30°

Q = 425 m³/min

	East				Lateral Position					West	
v_∞	x	z	42.5m	30m	20m	10m	₵	10m	22.5m	32.5m
2 mps	150m	G	0	0	0	0	4	0	0	0
	300m	G	8	4	4	7	9	9	8	7
	300m	30m	23	12	35	65	33	20	0	10
	300m	60m	407	315	830	1044	716	348	36	100
4 mps	150m	G	18	34	29	40	34	31	19	10
	300m	G	97	91	101	114	110	72	74	45
	300m	30m	152	224	274	284	290	155	56	60
	300m	60m	96	304	456	647	608	285	87	67
6 mps	150m	G	89	82	108	131	125	97	52	39
	300m	G	177	162	164	195	184	226	127	136
	300m	$3\frac{1}{2}$m	172	226	313	280	269	183	90	72
	300m	60m	46	66	104	118	138	108	60	31
8 mps	300m	G	140	120	105	131	132	126	57	51
	300m	G	167	170	198	234	238	217	169	170
	300m	G	164	144	187	207	198	167	116	93
	300m	G	33	63	67	88	101	74	36	29
10 mps	300m	G	112	96	123	152	116	97	58	42
	300m	G	160	164	150	200	189	181	132	101
	300m	G	104	110	137	166	154	100	–	53
	300m	G	15	13	32	56	48	43	26	30

TABLE 5 (continued)

Concentration Data

v_s = 60.8 mps

$0 = -30°$

$Q = 1700 \ m^3/min$

			East				Lateral Position		West	
v_∞	x	z	42.5m	30m	20m	10m	₵	10m	22.5m	32.5m
4 mps	500m	G	0	0	0	0	0	0	0	-
	1000m	G	0	0	0	0	0	0	0	-
	1000m	½m	11	15	29	13	25	40	-	-
	1000m	1m	0	20	11	28	30	63	9	-
8 mps	500m	G	19	38	25	27	20	22	20	0
	1000m	G	47	64	32	40	37	40	31	-
	1000m	½m	175	202	212	226	156	88	65	14
	1000m	1m	600	654	854	1023	661	216	65	40
15 mps	500m	G	30	32	27	32	28	20	30	10
	1000m	G	99	81	97	107	49	82	55	24
	1000m	½m	282	301	358	365	309	165	82	52
	1000m	1m	313	300	585	796	537	265	77	60
20 mps	500m	G	33	30	36	25	23	25	22	14
	1000m	G	117	85	85	102	105	59	48	46
	1000m	½m	271	290	370	400	253	146	-	65
	1000m	1m	139	127	268	407	319	187	52	34
25 mps	500m	G	41	32	47	52	33	45	18	14
	1000m	G	117	109	133	149	95	85	55	19
	1000m	½m	278	274	348	366	230	130	39	26
	1000m	1m	40	69	113	194	154	68	25	24

FIGURES

PLAN VIEW
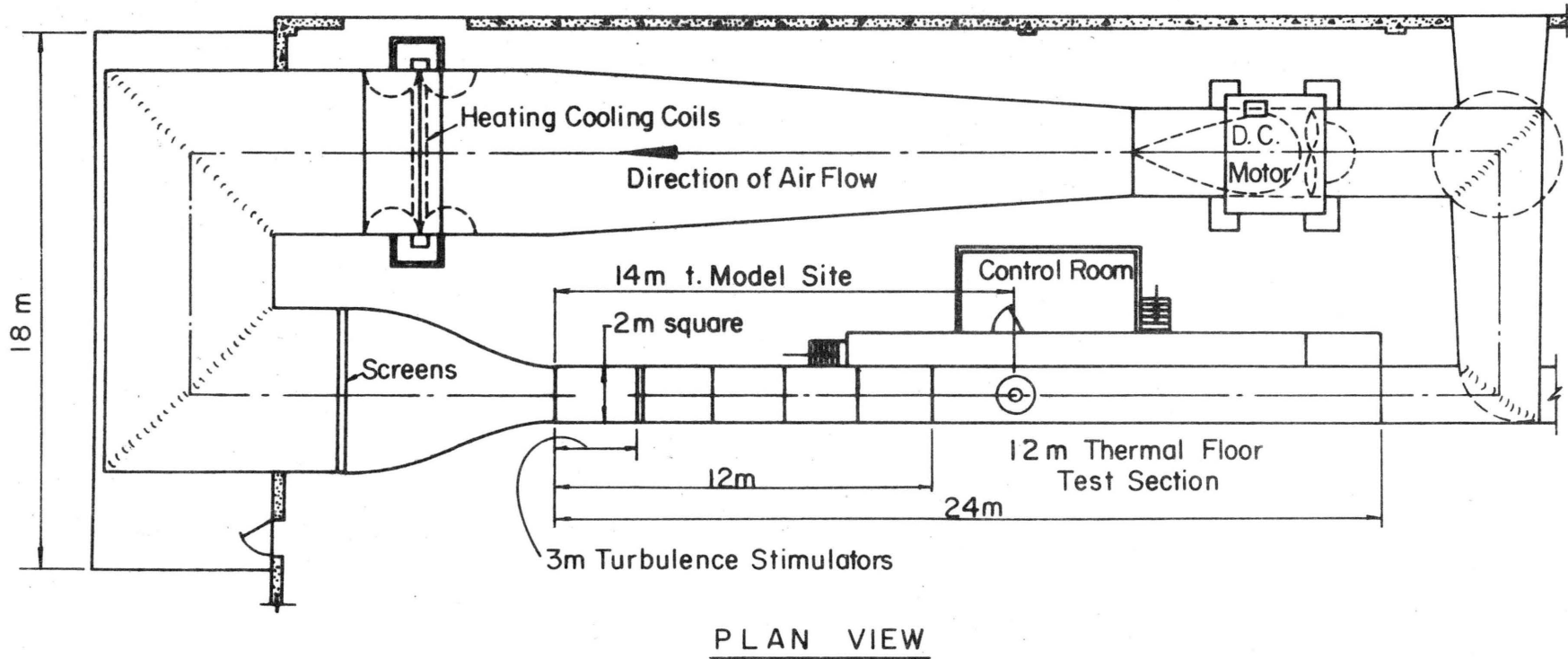
Fig. 1. Army Meteorological Wind Tunnel
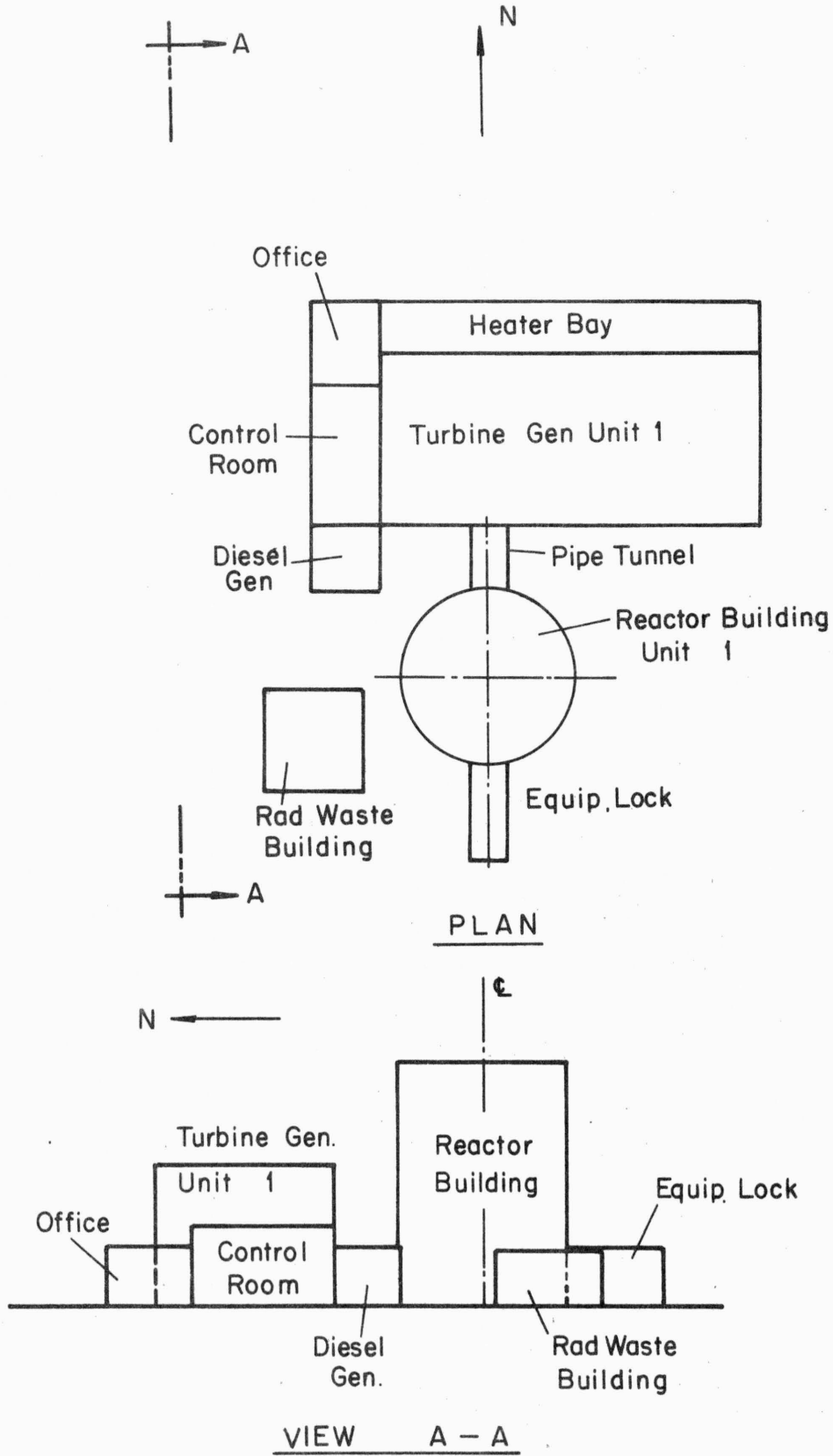
Fig. 2. Shoreham Nuclear Reactor Complex

Uniform Flow

Streamlines

Cavity

Upstream Cavity

Stagnation Point of Cavity

Separation Point

Wake Boundary

Stagnation Point

Cavity Boundary

Stagnation Point
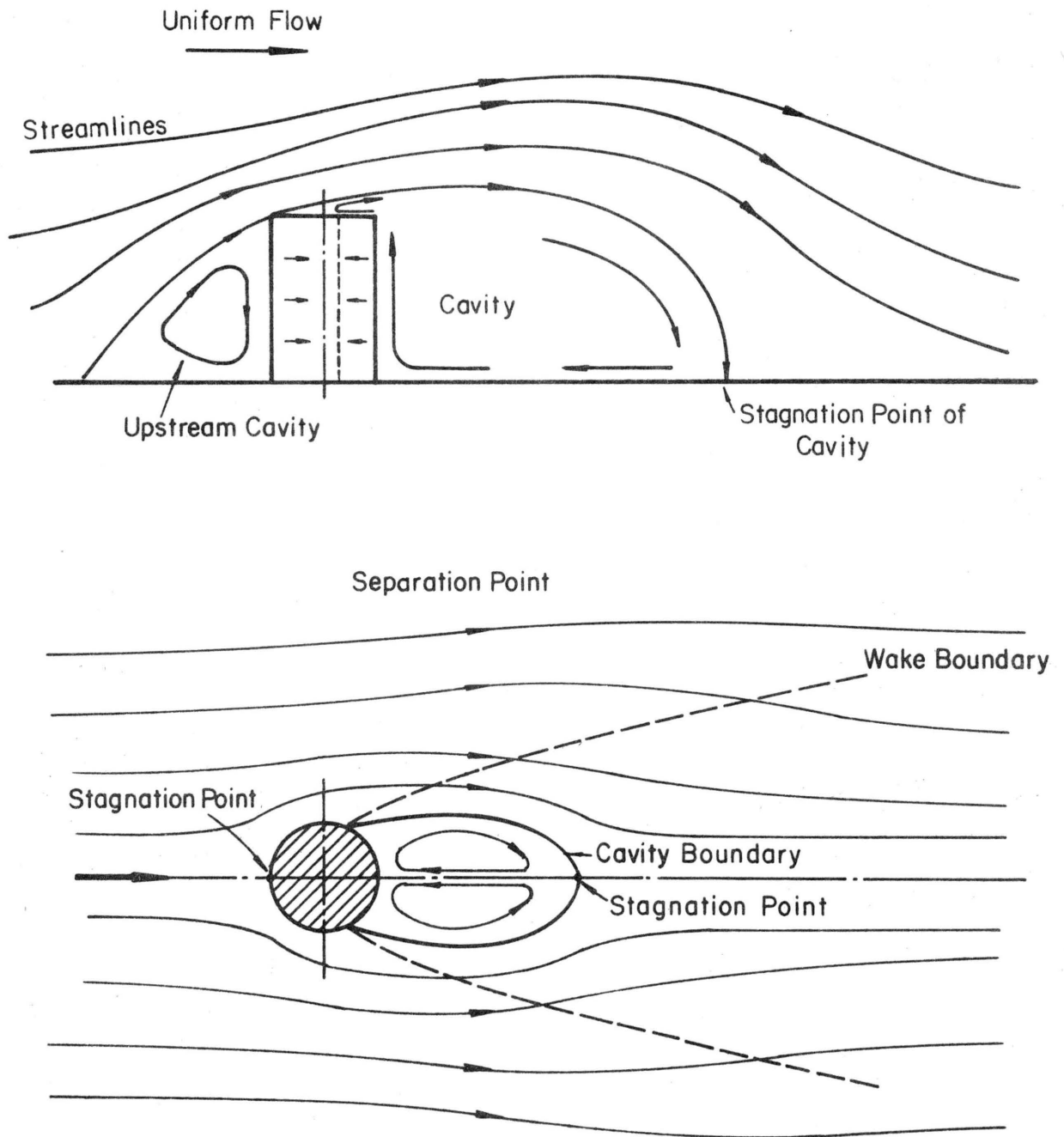
Fig. 3a. Cavity and Wake Downstream of a Circular Building
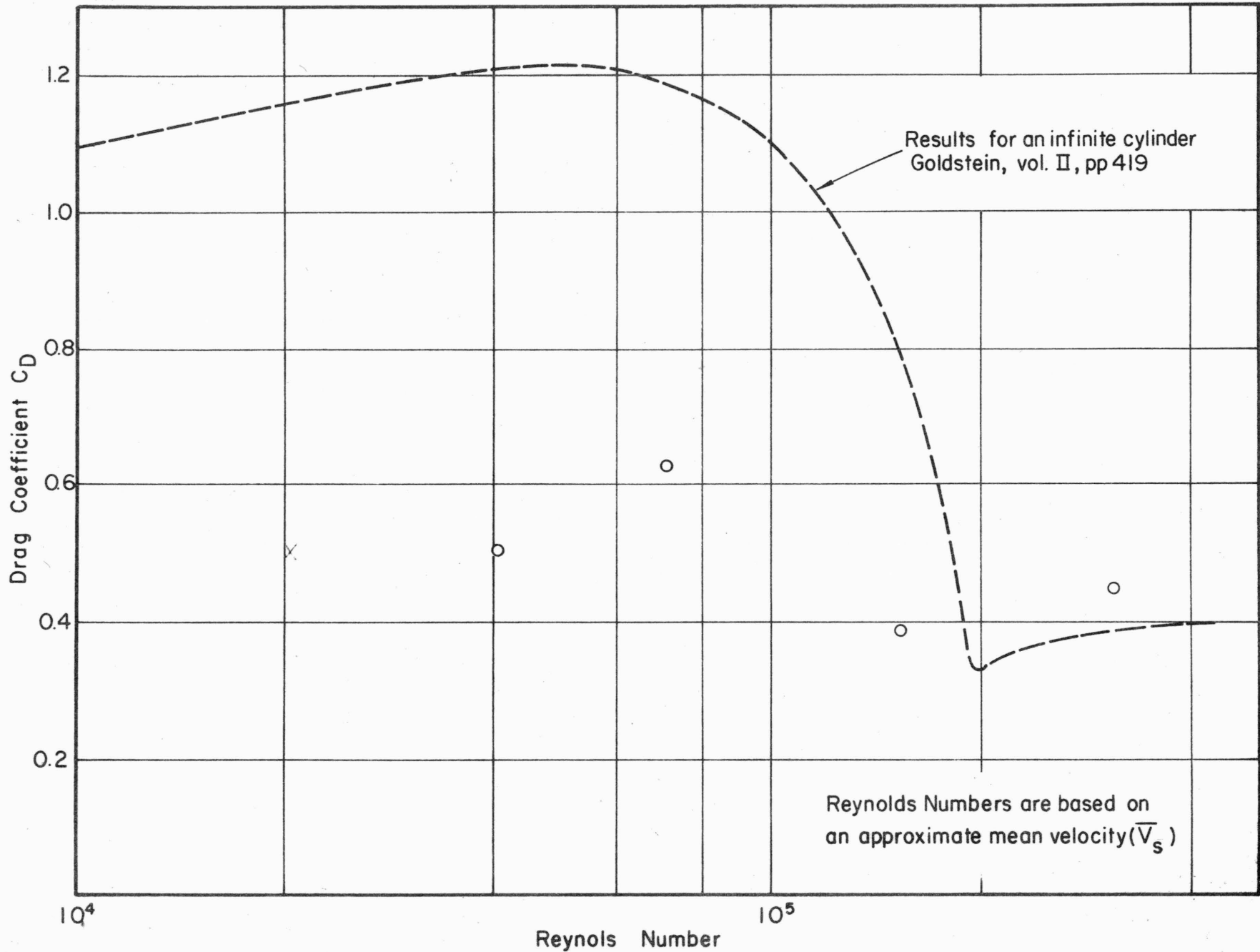
Fig. 3b. Drag Force Measurements

The plot shows Drag Coefficient C_D (vertical axis) versus Reynolds Number (horizontal axis, logarithmic from 10^4 to beyond 10^5).

Results for an infinite cylinder
Goldstein, vol. II, pp 419

Reynolds Numbers are based on
an approximate mean velocity $(\overline{V}_s)$

33
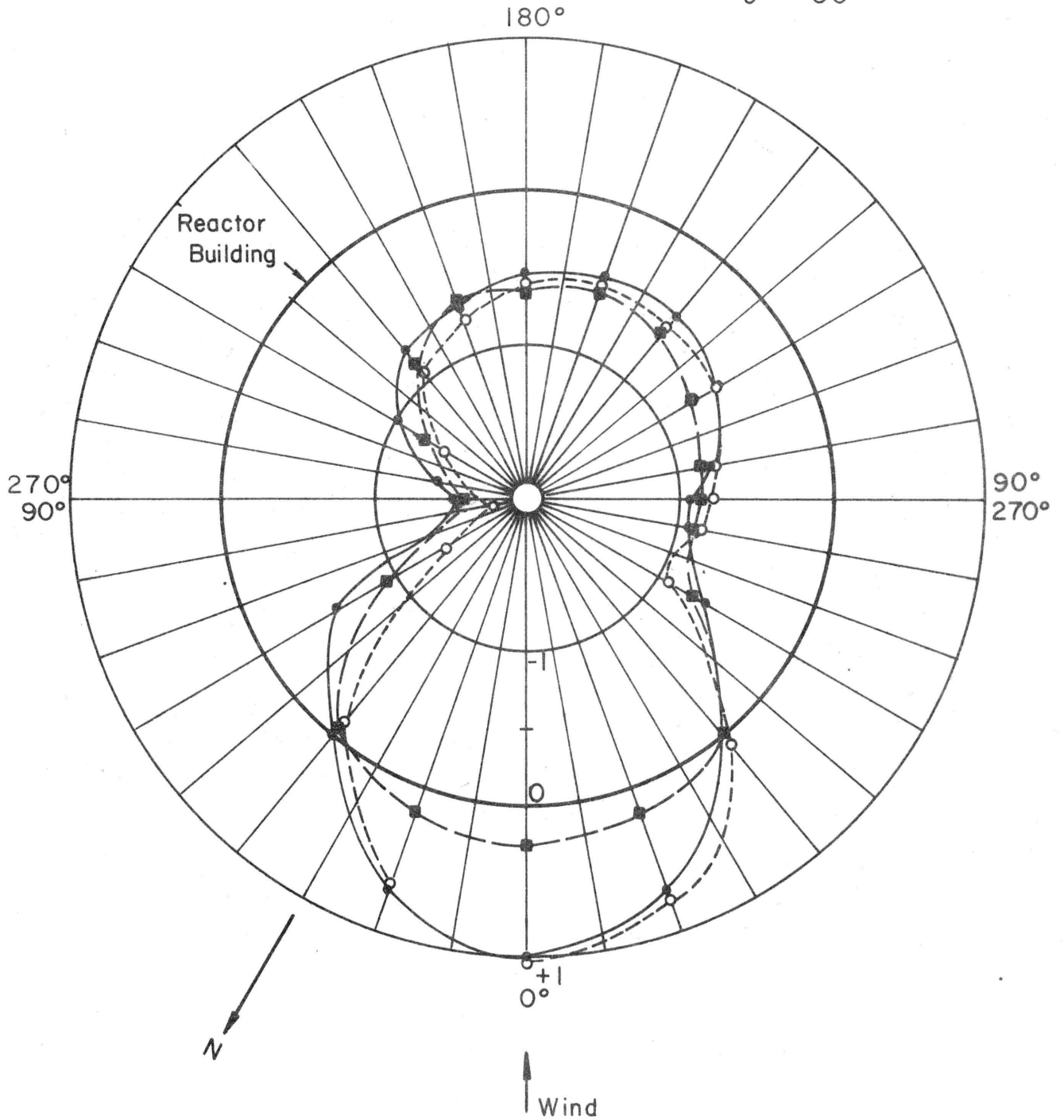
Fig. 4a. Static Pressure Distribution about Containment Vessels
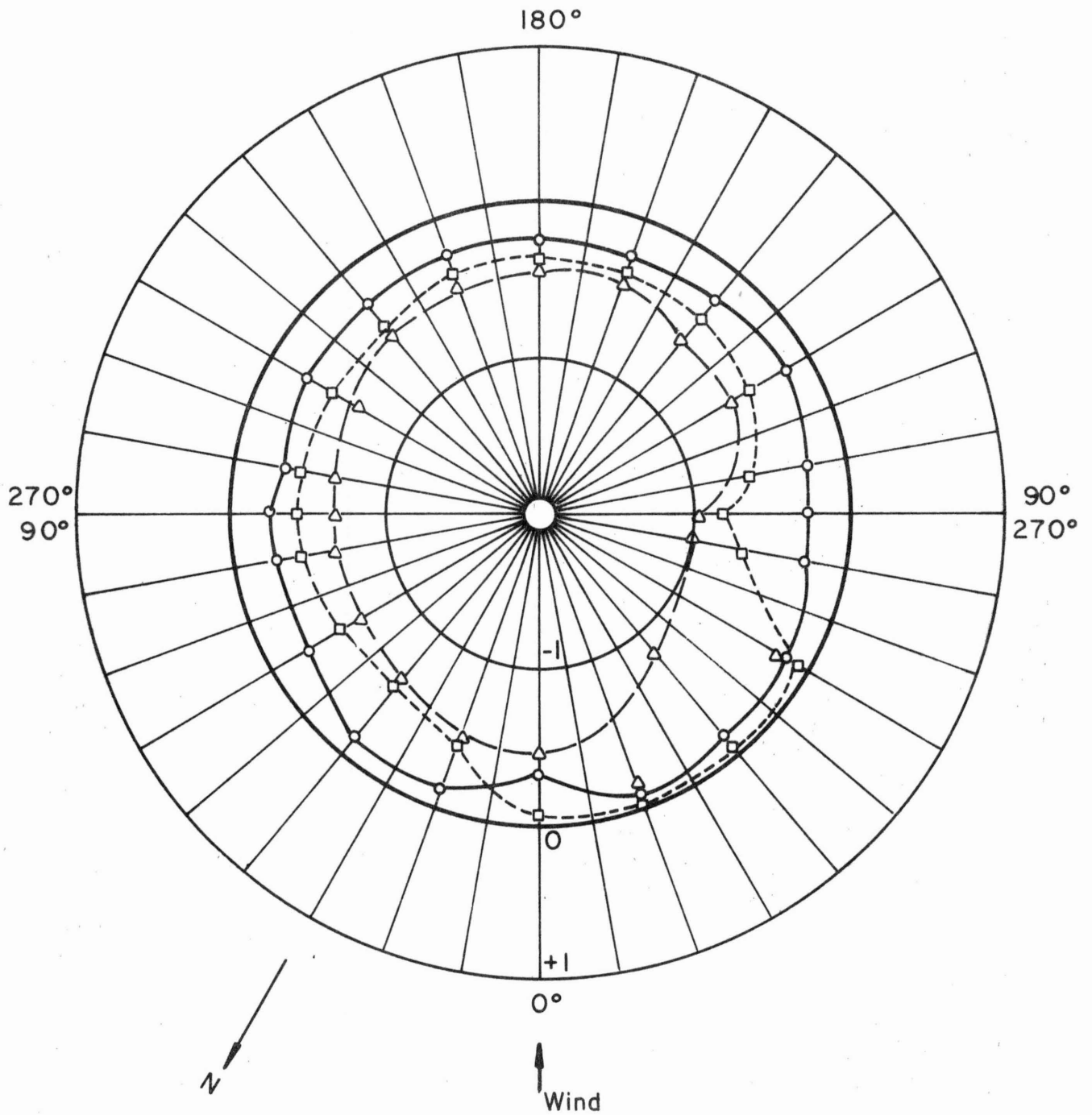
Fig. 4b.   Static Pressure Distribution about Containment Vessels
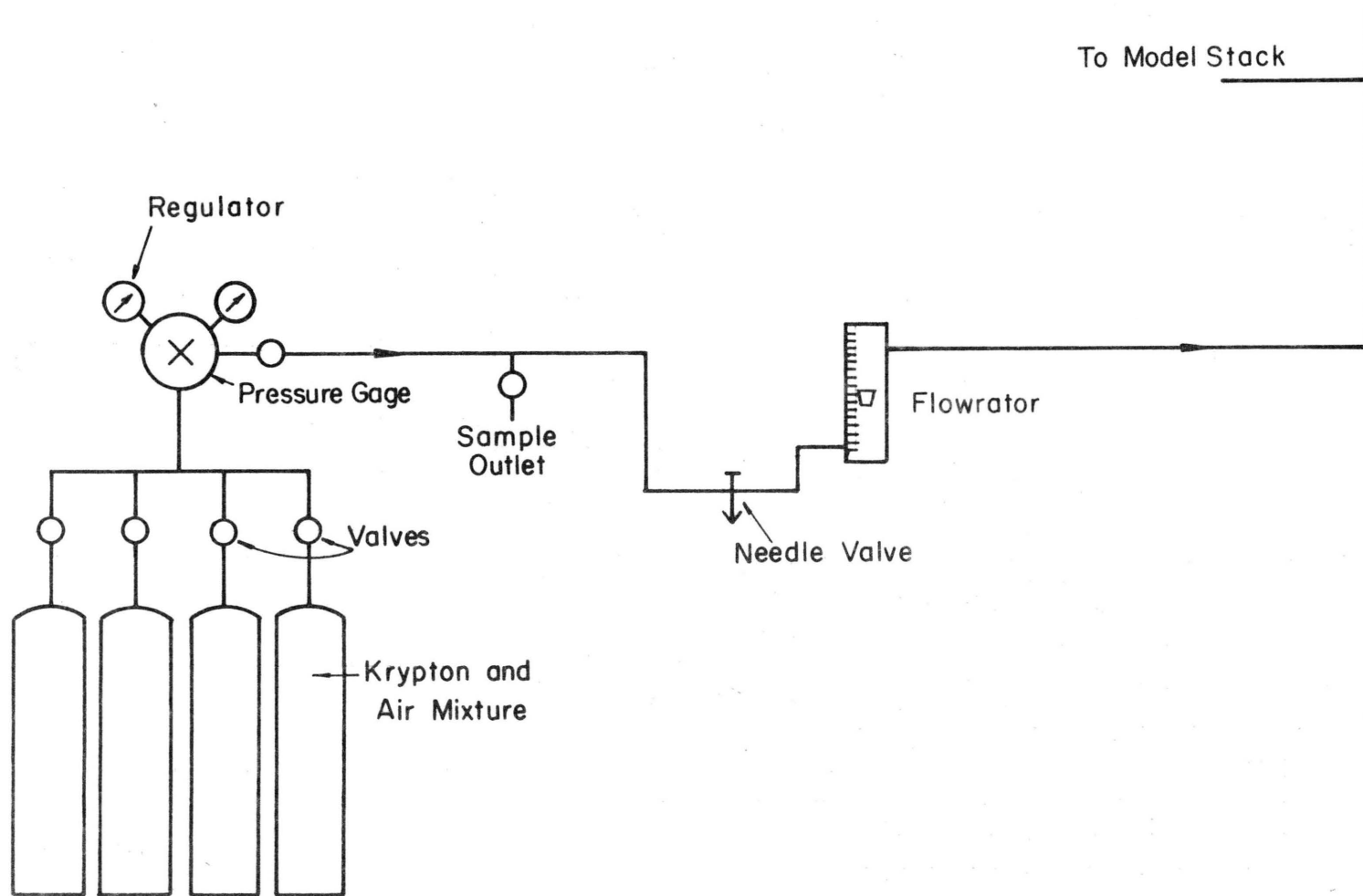
Fig. 5a. Gas Tracer Apparatus
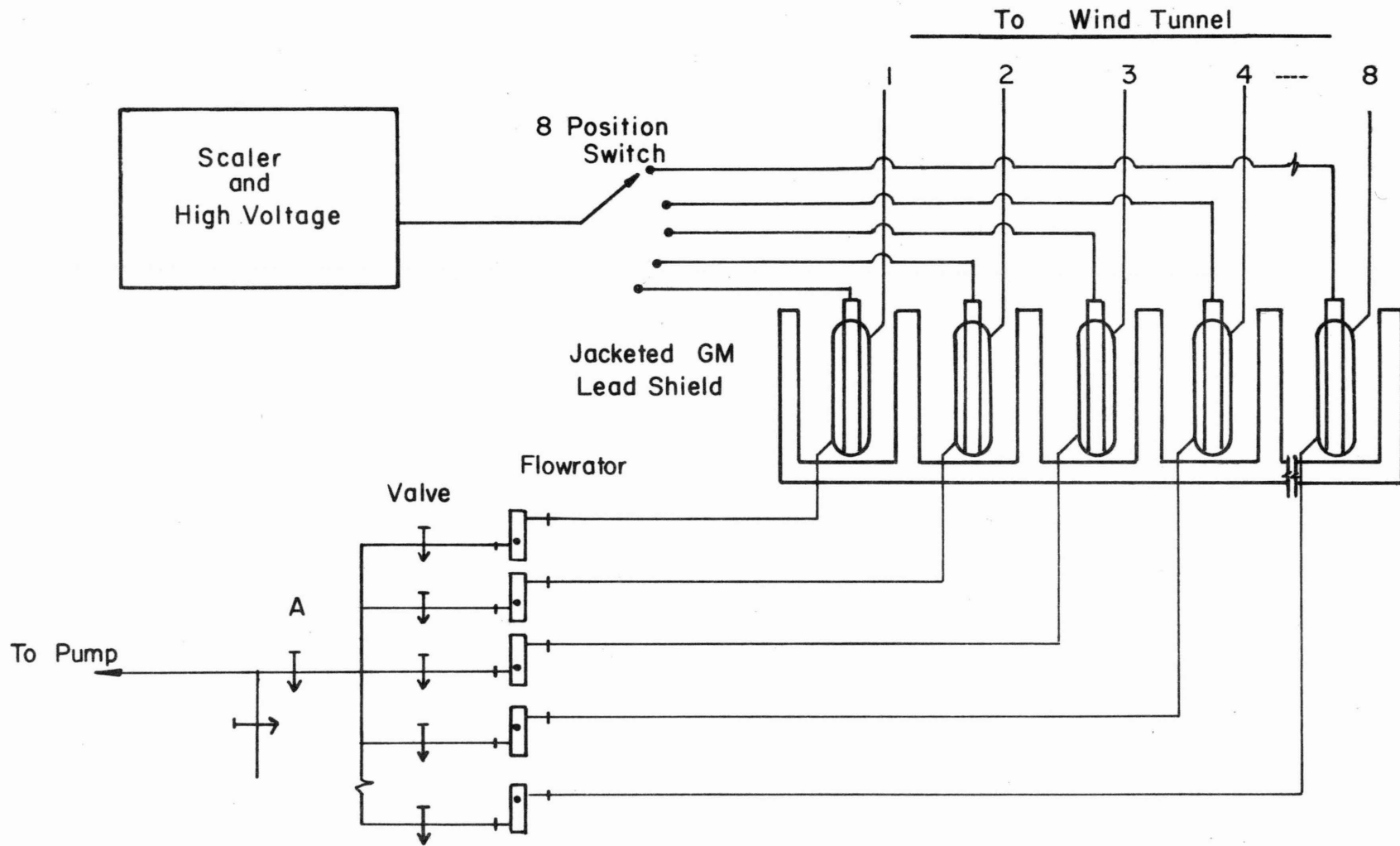
Fig. 5b. Gas Tracer Apparatus
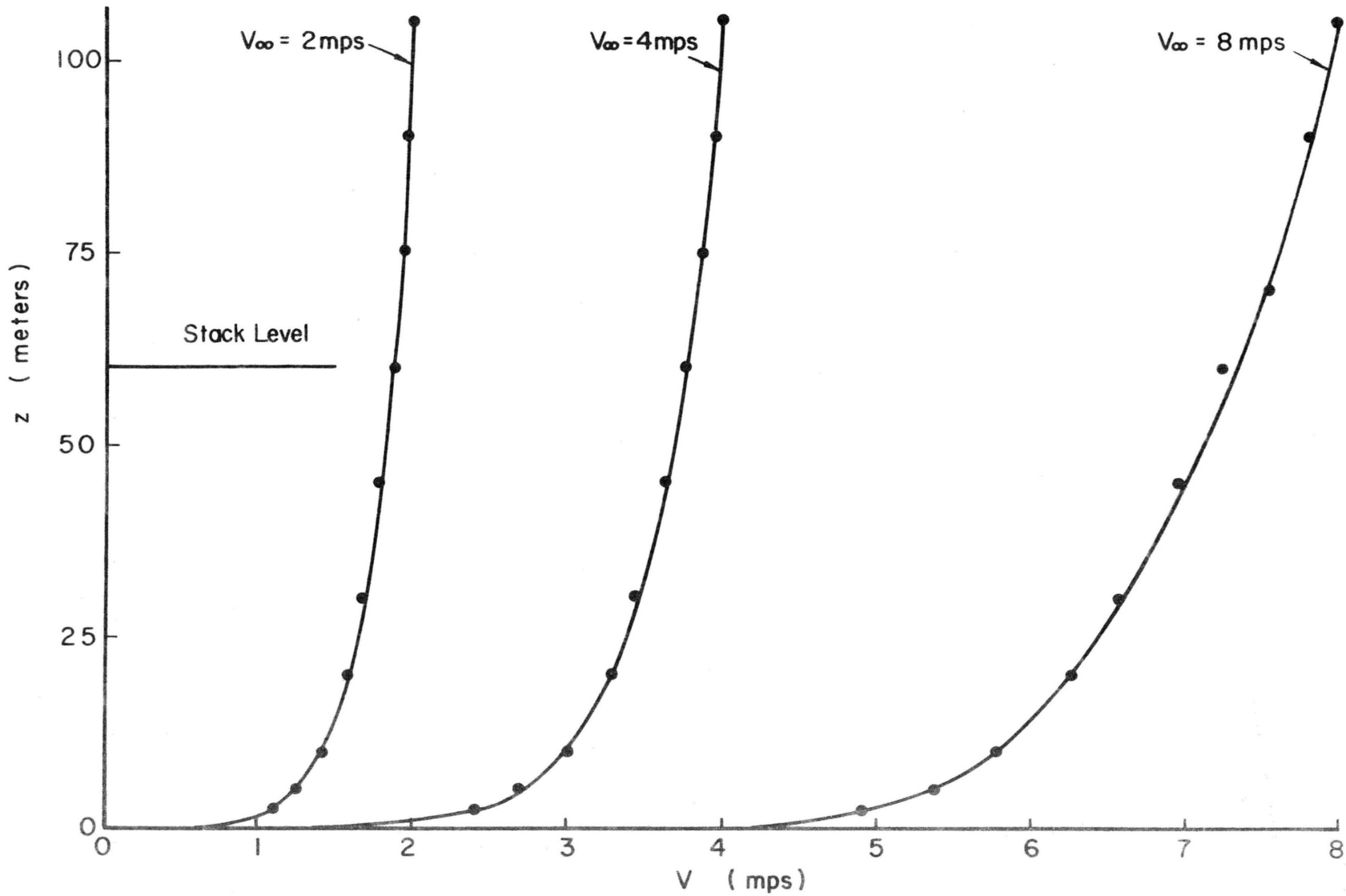
Fig. 6a. Upstream Velocity Profiles
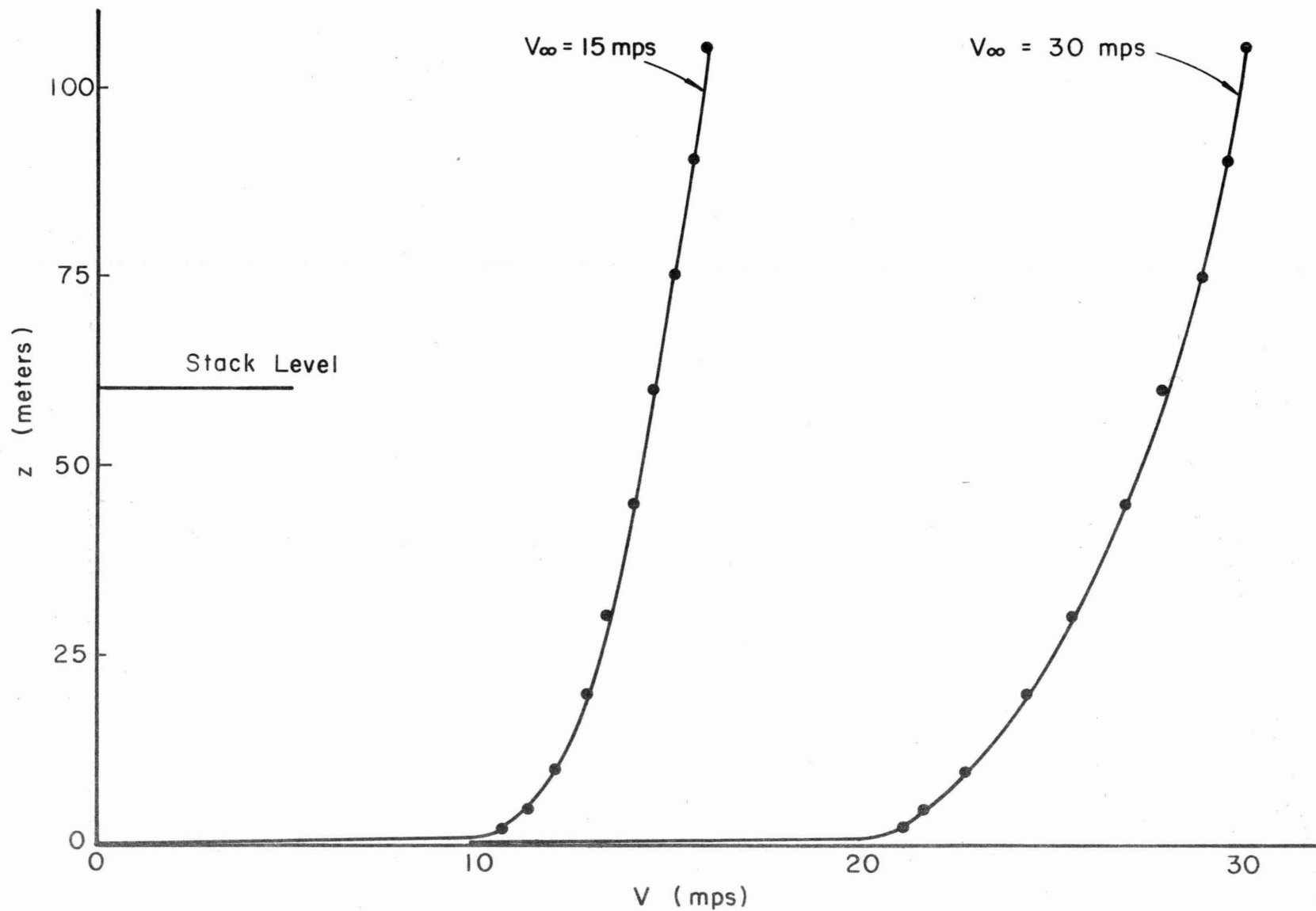
Fig. 6b. Upstream Velocity Profiles

38
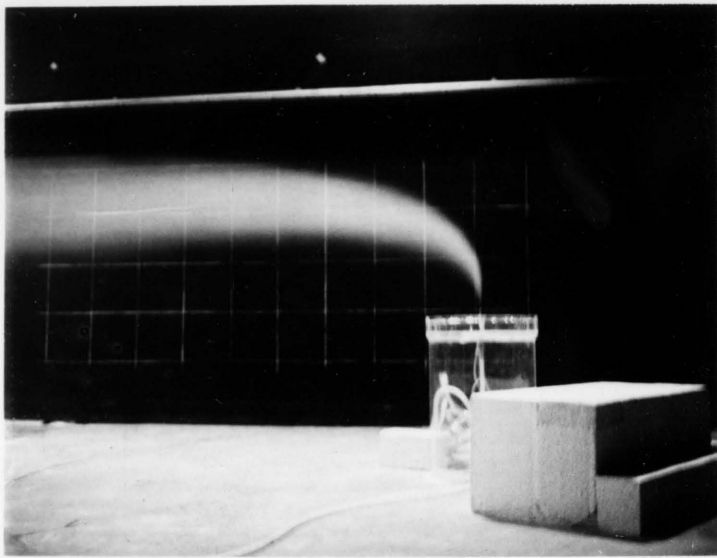
$U_\infty = 1$ m/sec
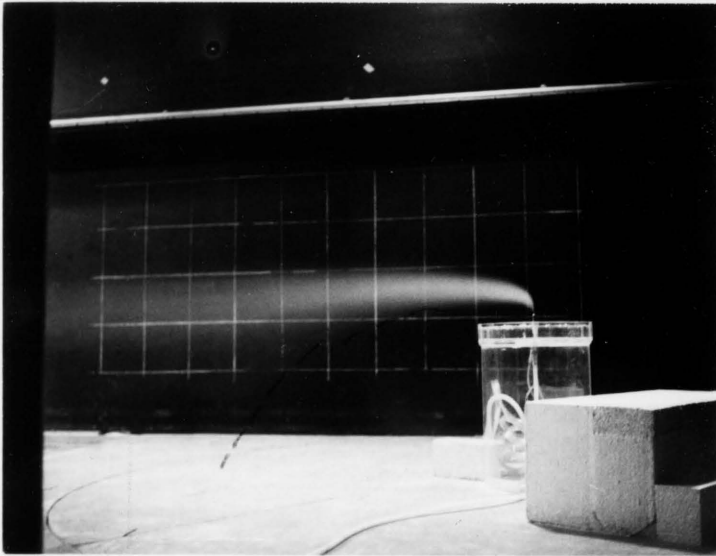
$U_\infty = 2$ m/sec

$U_\infty = 4$ m/sec
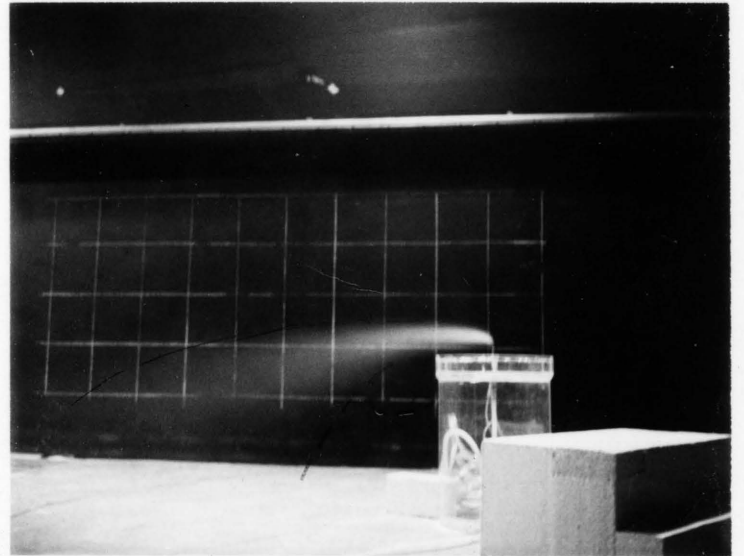
$U_\infty = 6$ m/sec

$V = 15.2$ m/sec $\theta = 330°$

Fig. 7 Typical Smoke Plume Variation with Wind Speed
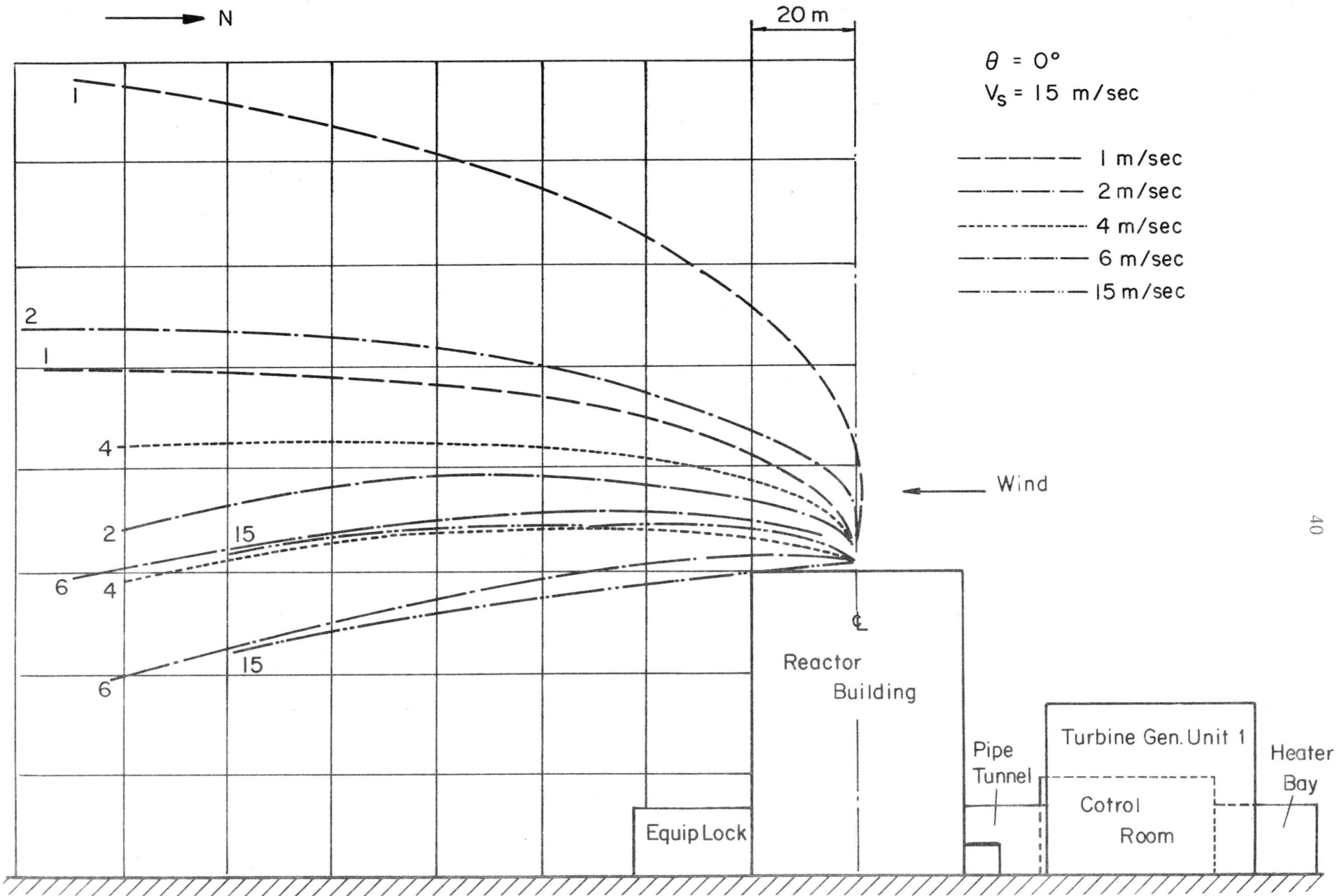
Fig. 8. Smoke Plume Sections for a Gas Stack,
Velocity of 15.2 mps, θ = 0
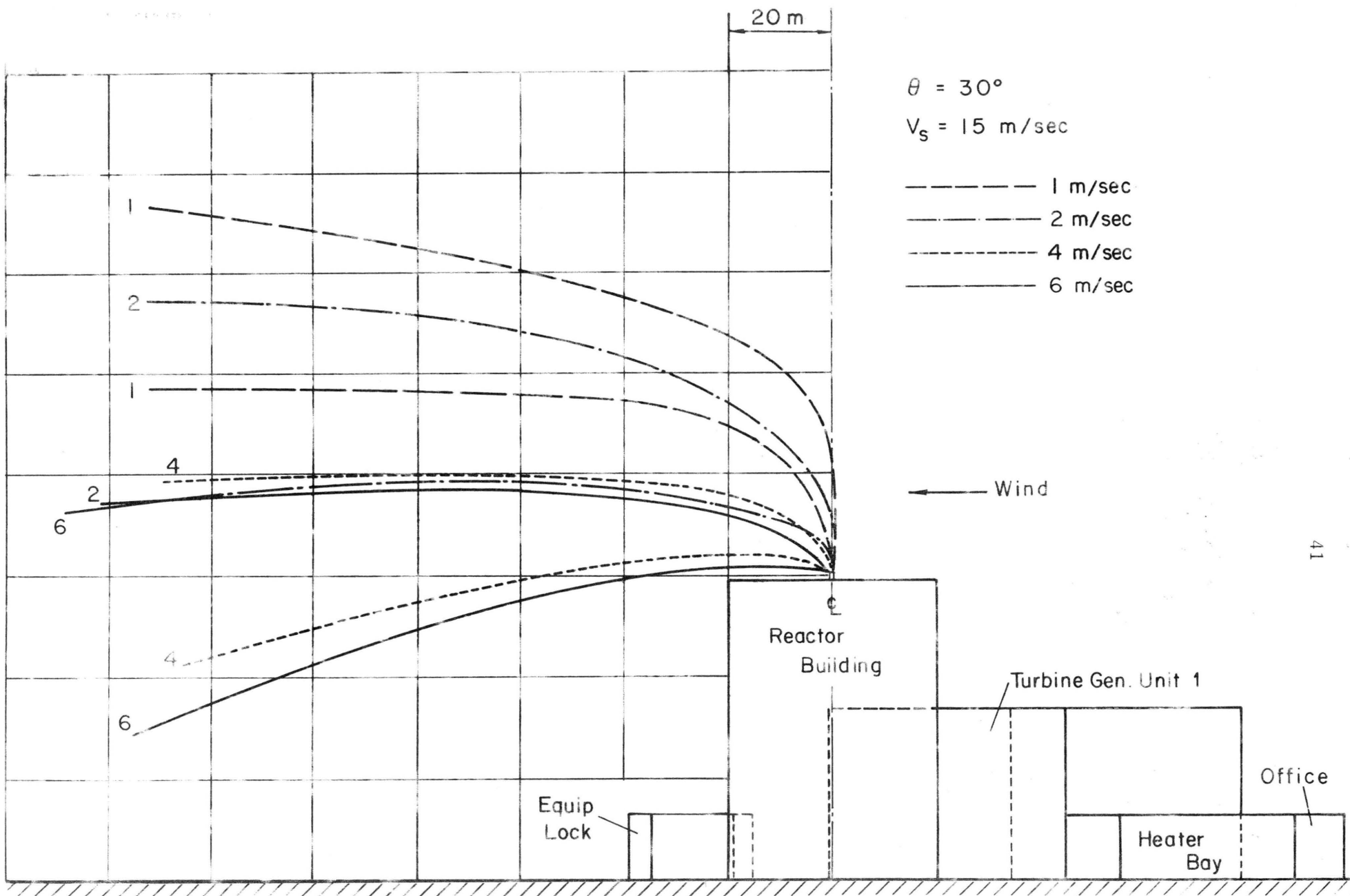
Fig. 9.   Smoke Plume Sections for a Gas Stack,
Velocity of 15.2 mps,   θ = 30°
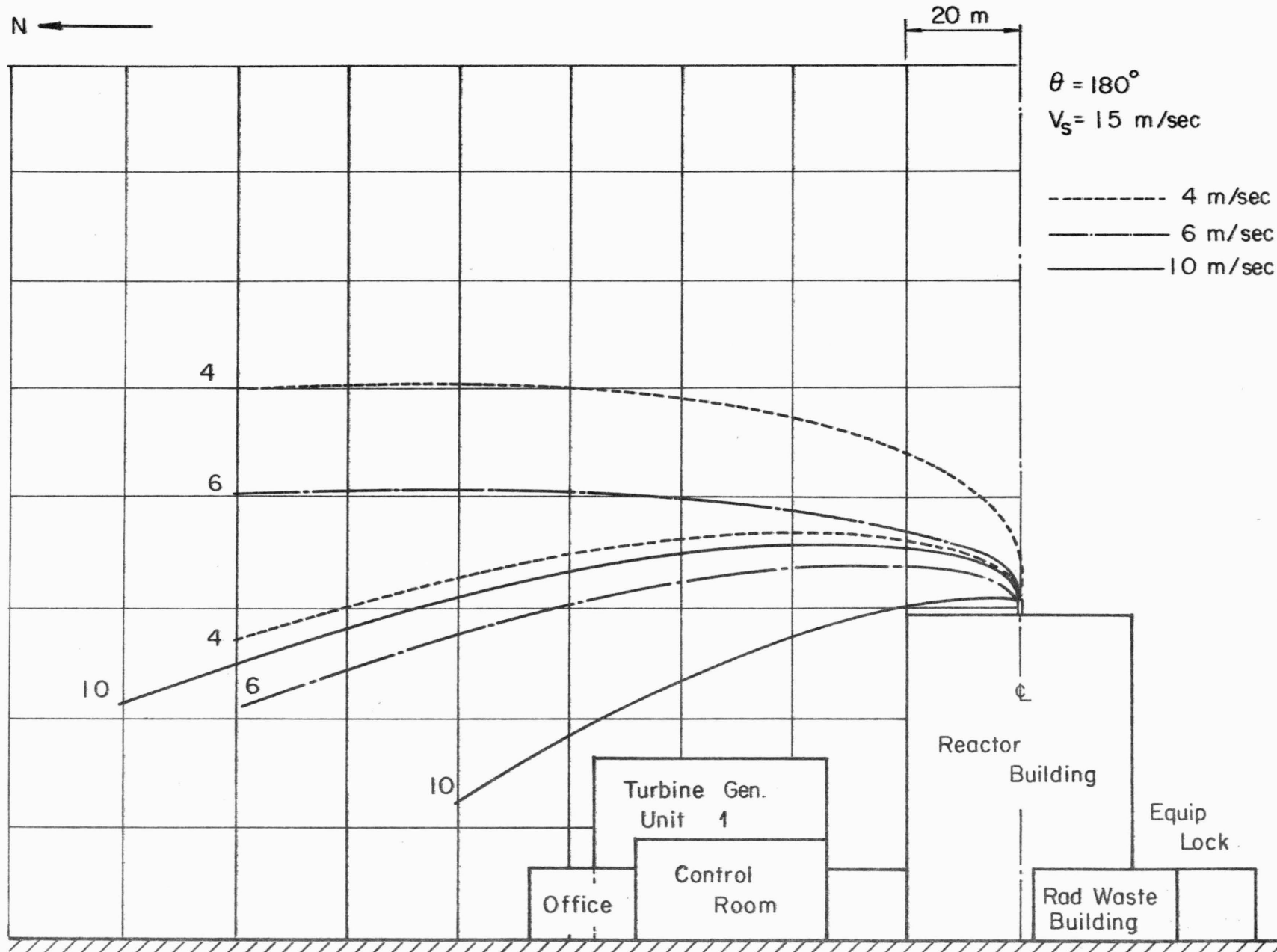
Fig. 10. Smoke Plume Sections for a Gas Stack,
Velocity of 15.2 mps, θ = 180°
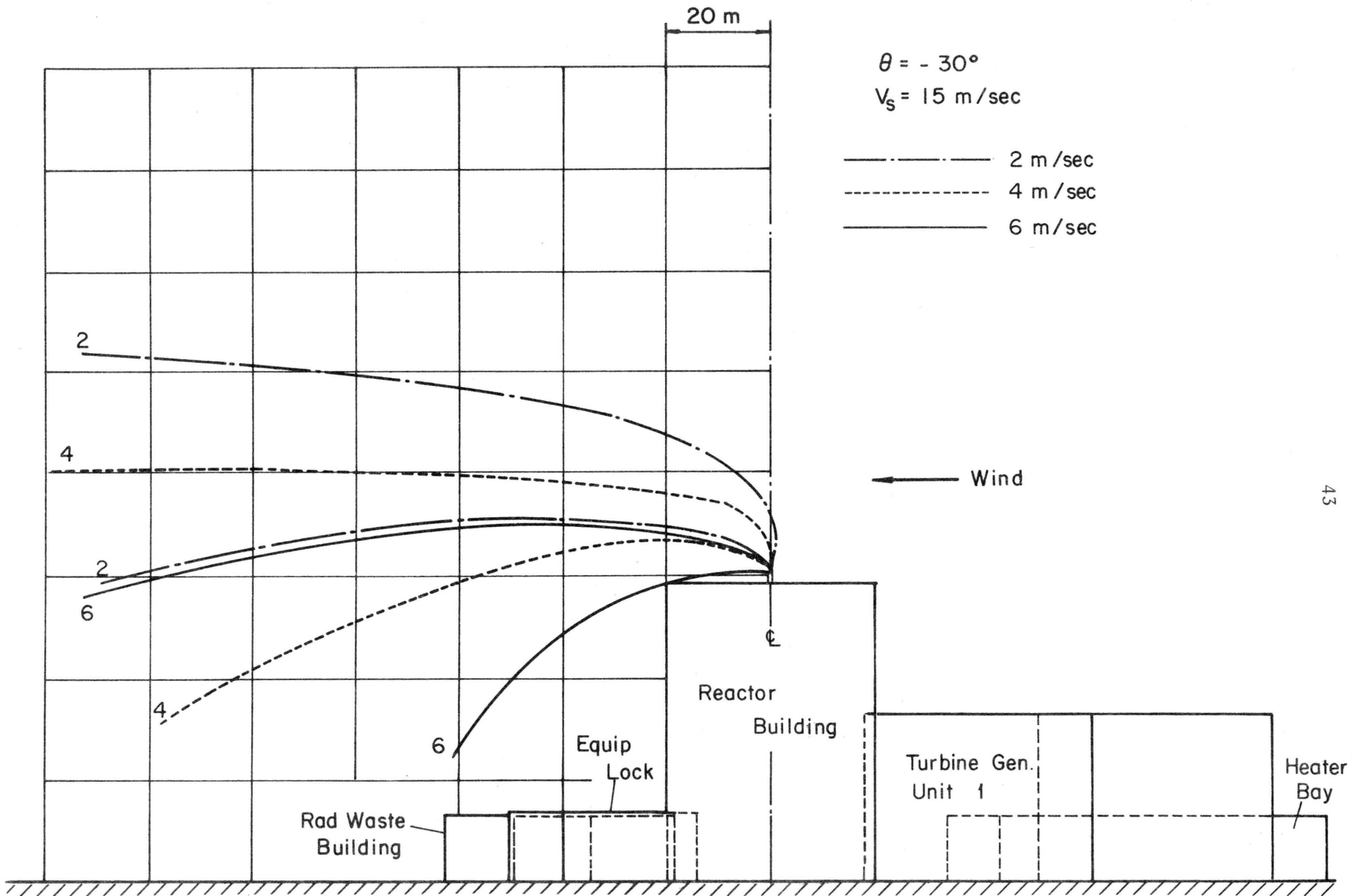
Fig. 11. Smoke Plume Sections for a Gas Stack,
Velocity of 15.2 mps, θ = - 30°
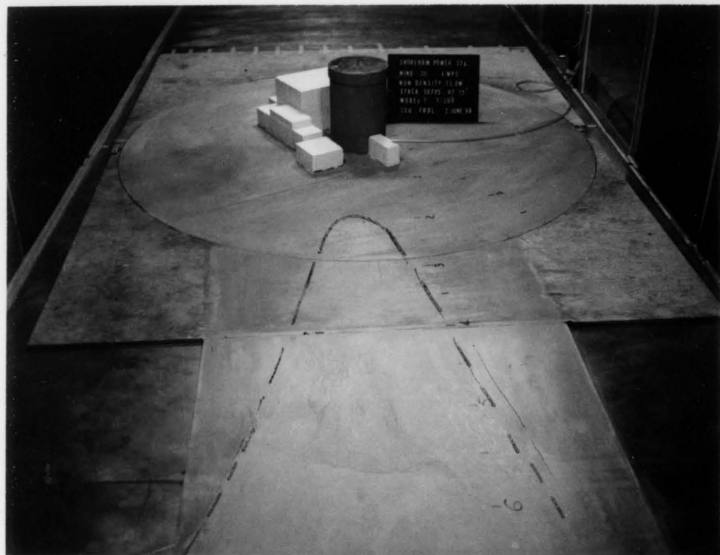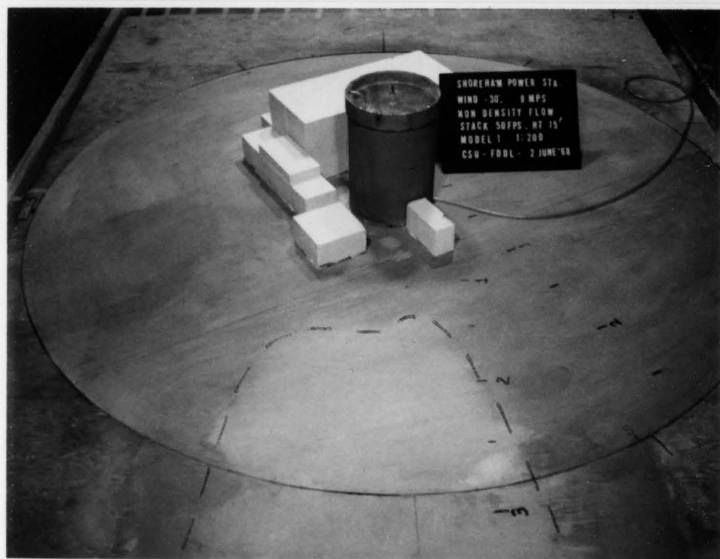
U∞ = 4 m / sec
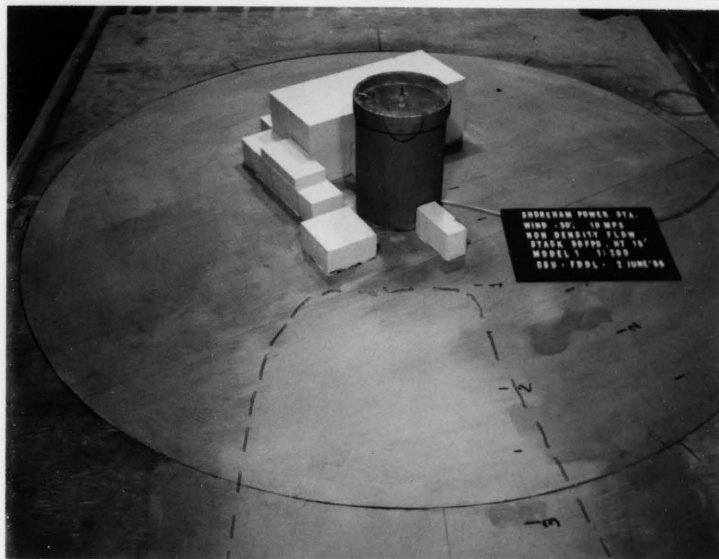
U∞ = 6 m / sec

U∞ = 8 m / sec

U∞ = 10 m / sec

V_S = 15.2 m/sec θ = 30°

Fig. 12   Ammonia Contact Traces, θ = 30°
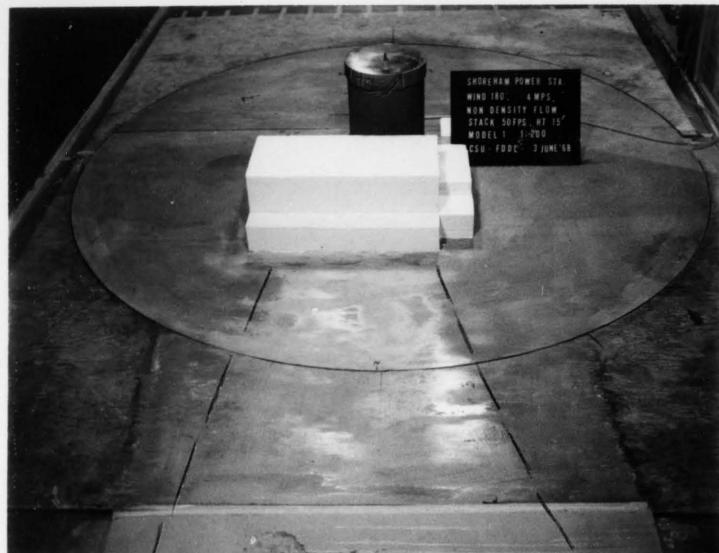
U∞ = 4 m/sec

U∞ = 6 m/sec

U∞ = 8 m/sec

V_s = 15.2 m/sec

θ = 180°

Fig. 13   Ammonia Contact Traces, θ = 180°
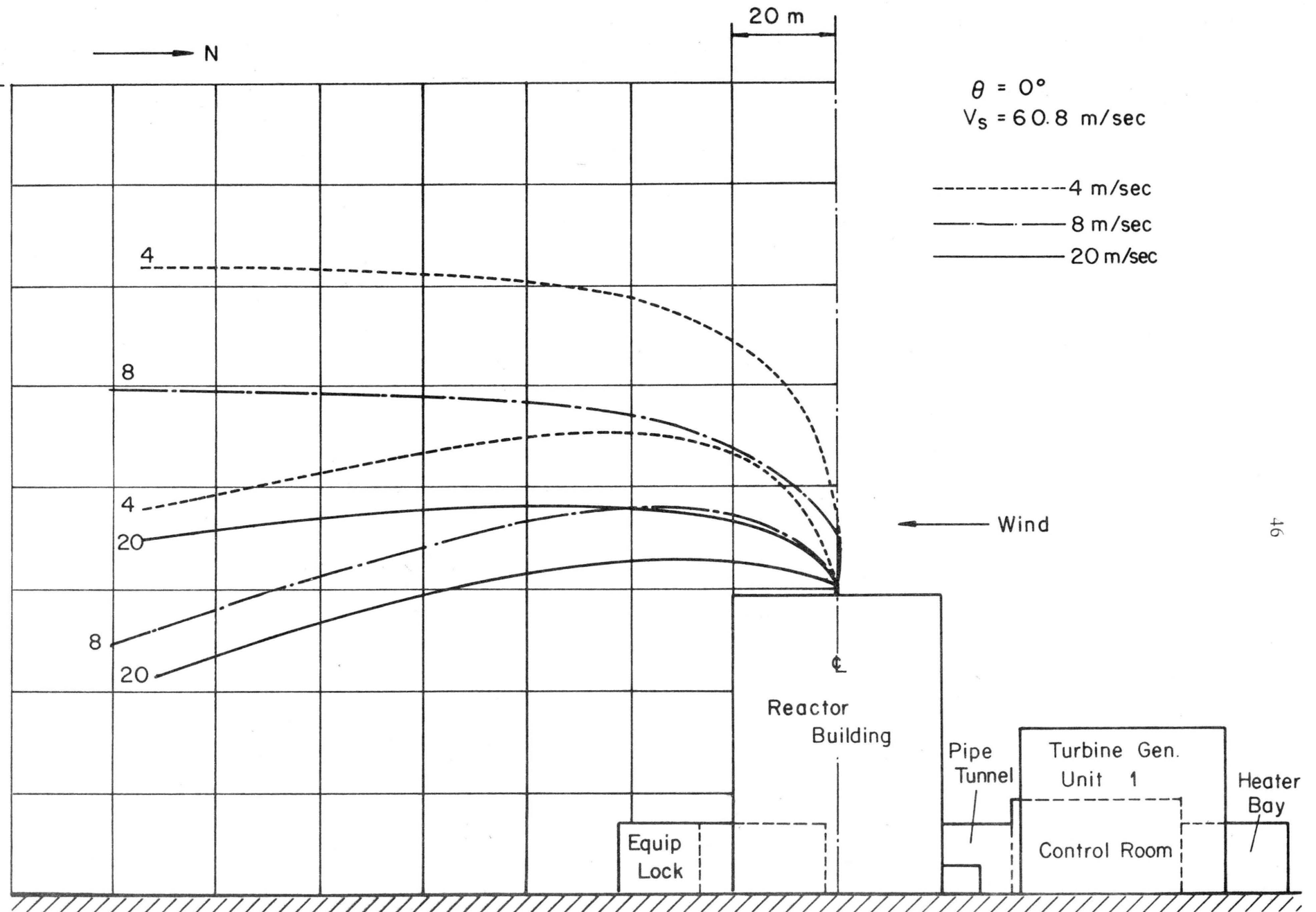
Fig. 14. Smoke Plume Sections for a Gas Stack,
Velocity of 60.8 mps, $\theta = 0°$
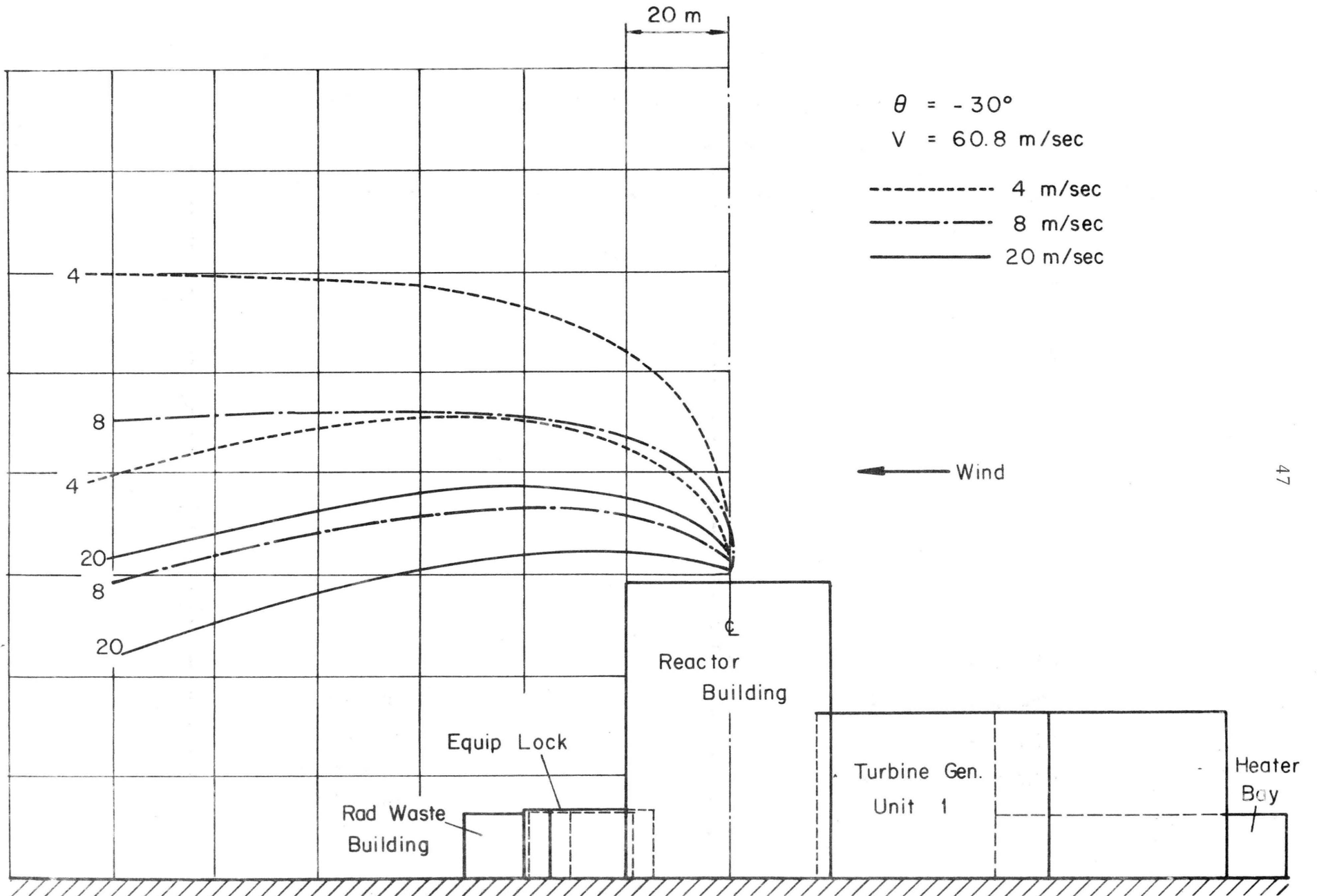
Fig. 15. Smoke Plume Sections for a Gas Stack,
Velocity of 60.8 mps, θ = - 30°
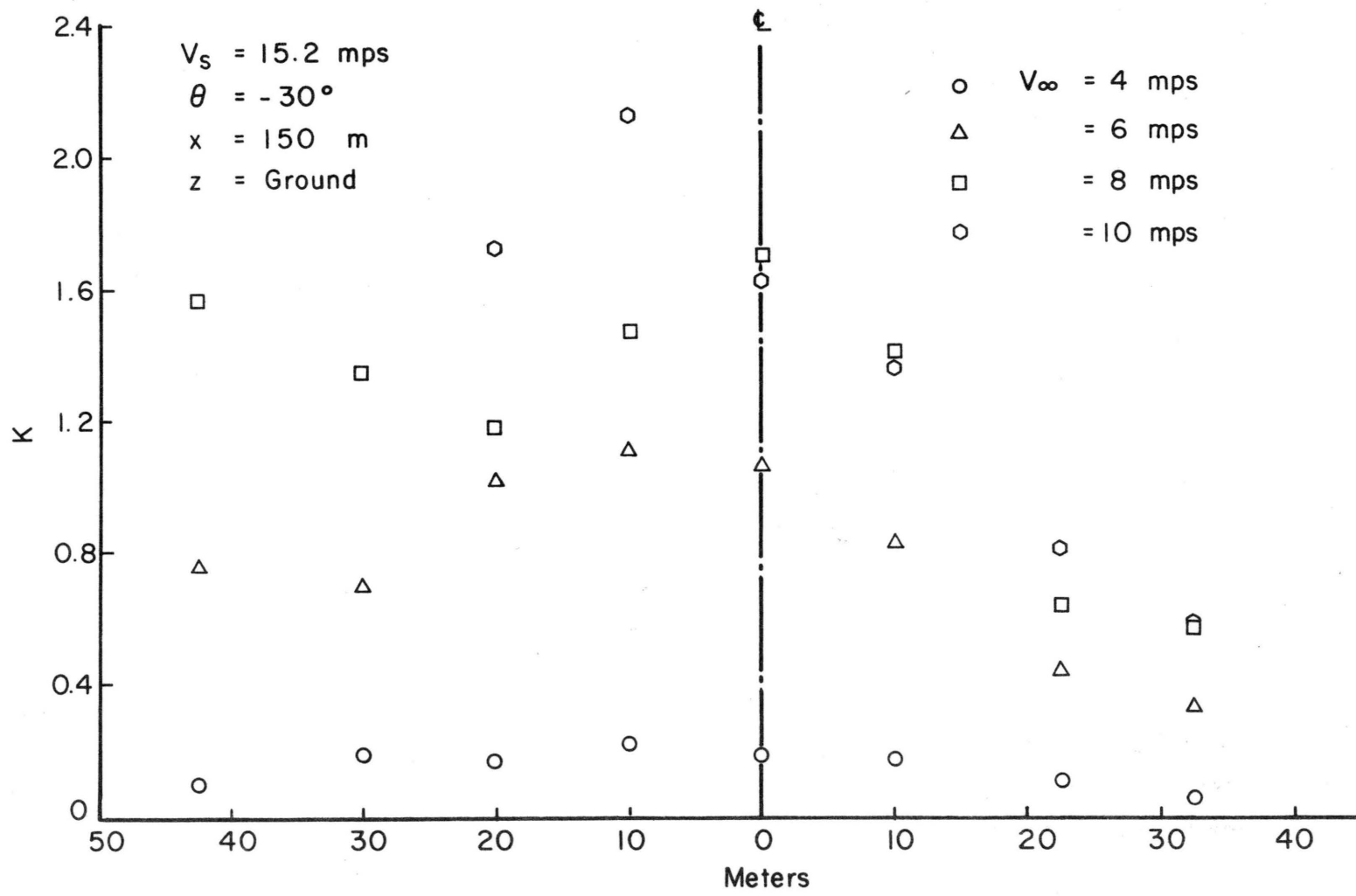
Fig. 16a. K-Profile for Gas Released at V_s = 15.2 mps,
θ = 330°, $\mathring{Q}$ = 425.0 m³/min

48
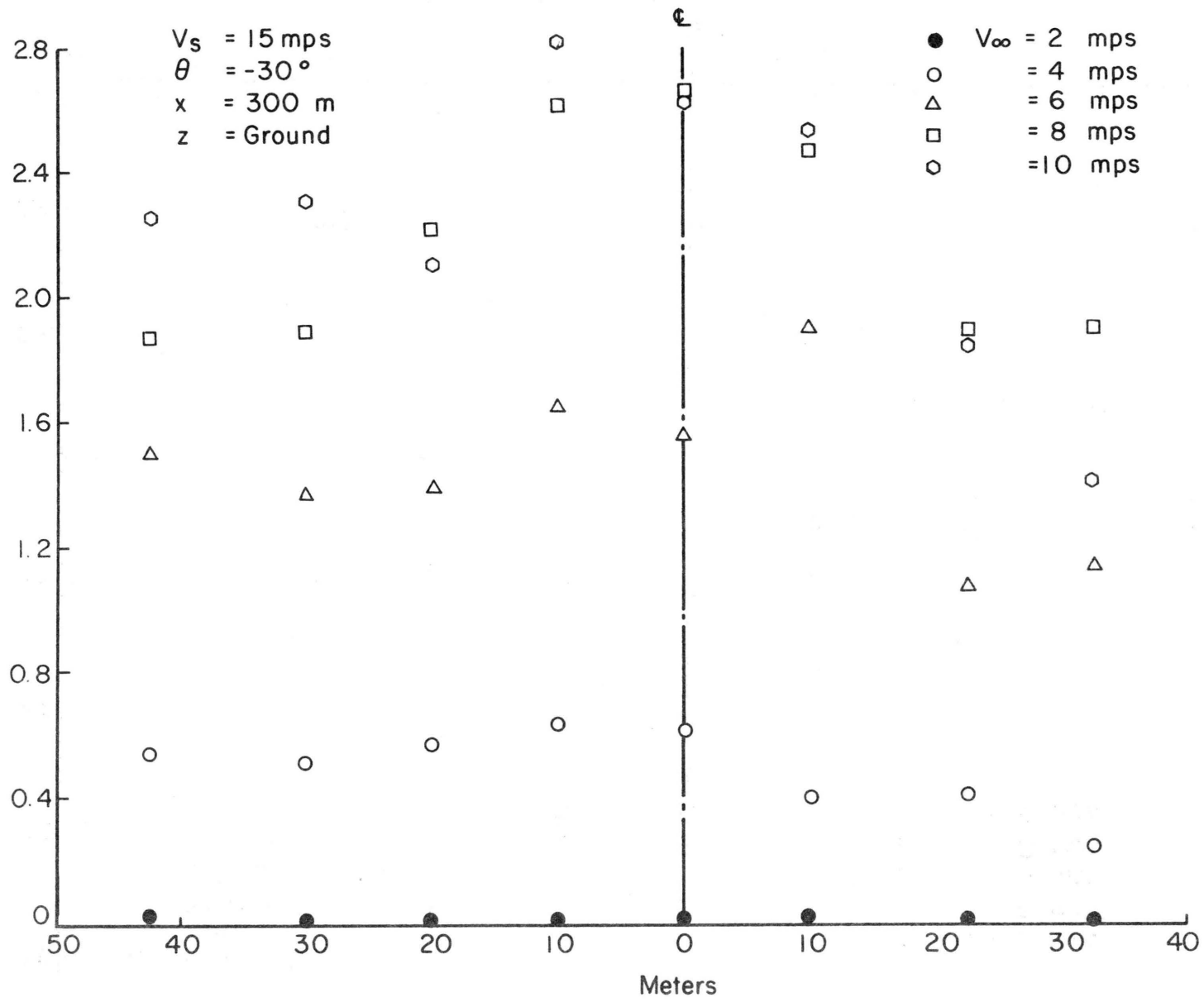
Fig. 16b. K-Profile for Gas Released at $V_s = 15.2$ mps,
$\theta = 330^O$, $\mathring{Q} = 425.0$ m^3/min
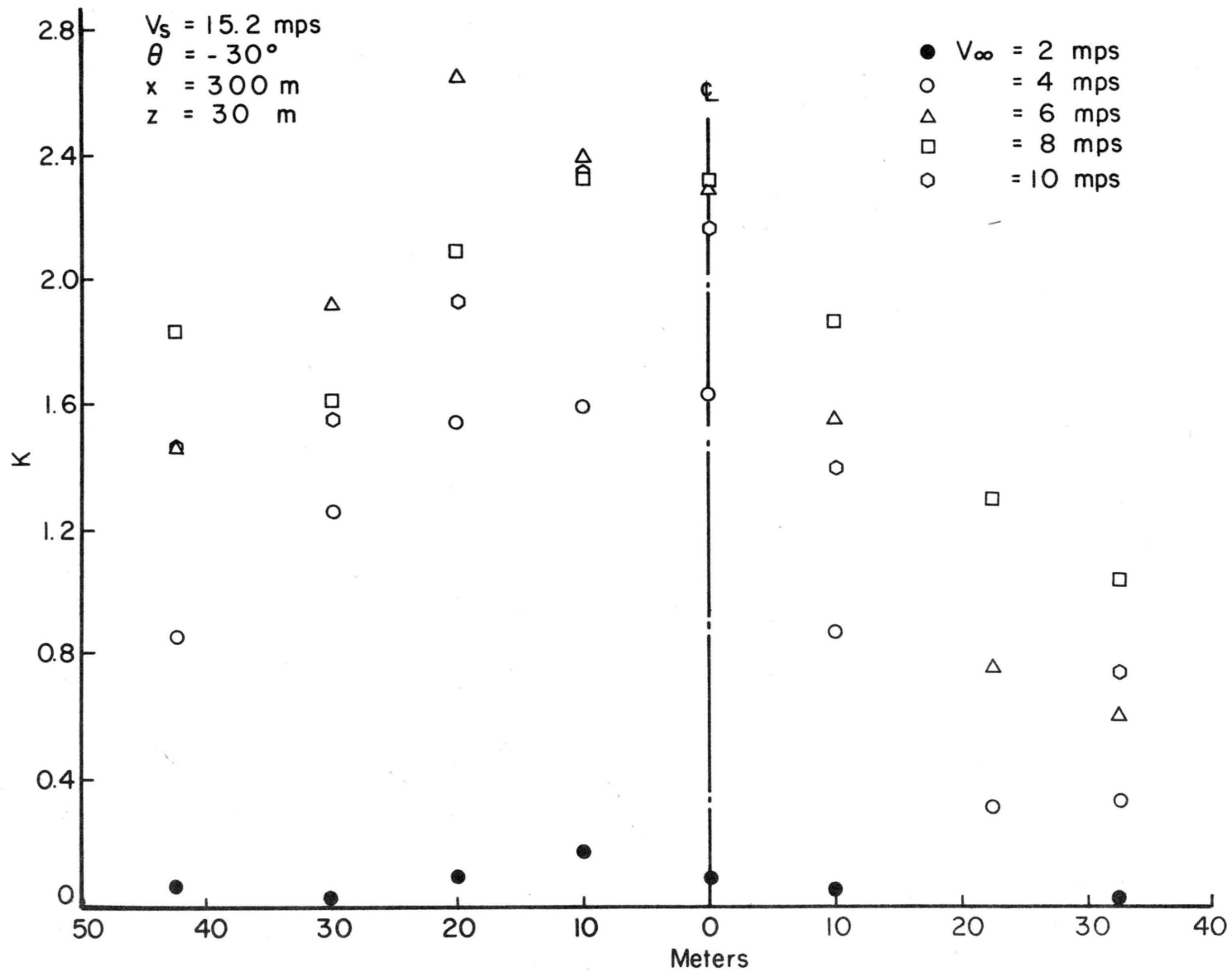
Fig. 16c. K-Profile for Gas Released at V_s = 15.2 mps, θ = 330°, $\overset{\circ}{Q}$ = 425.0 m³/min
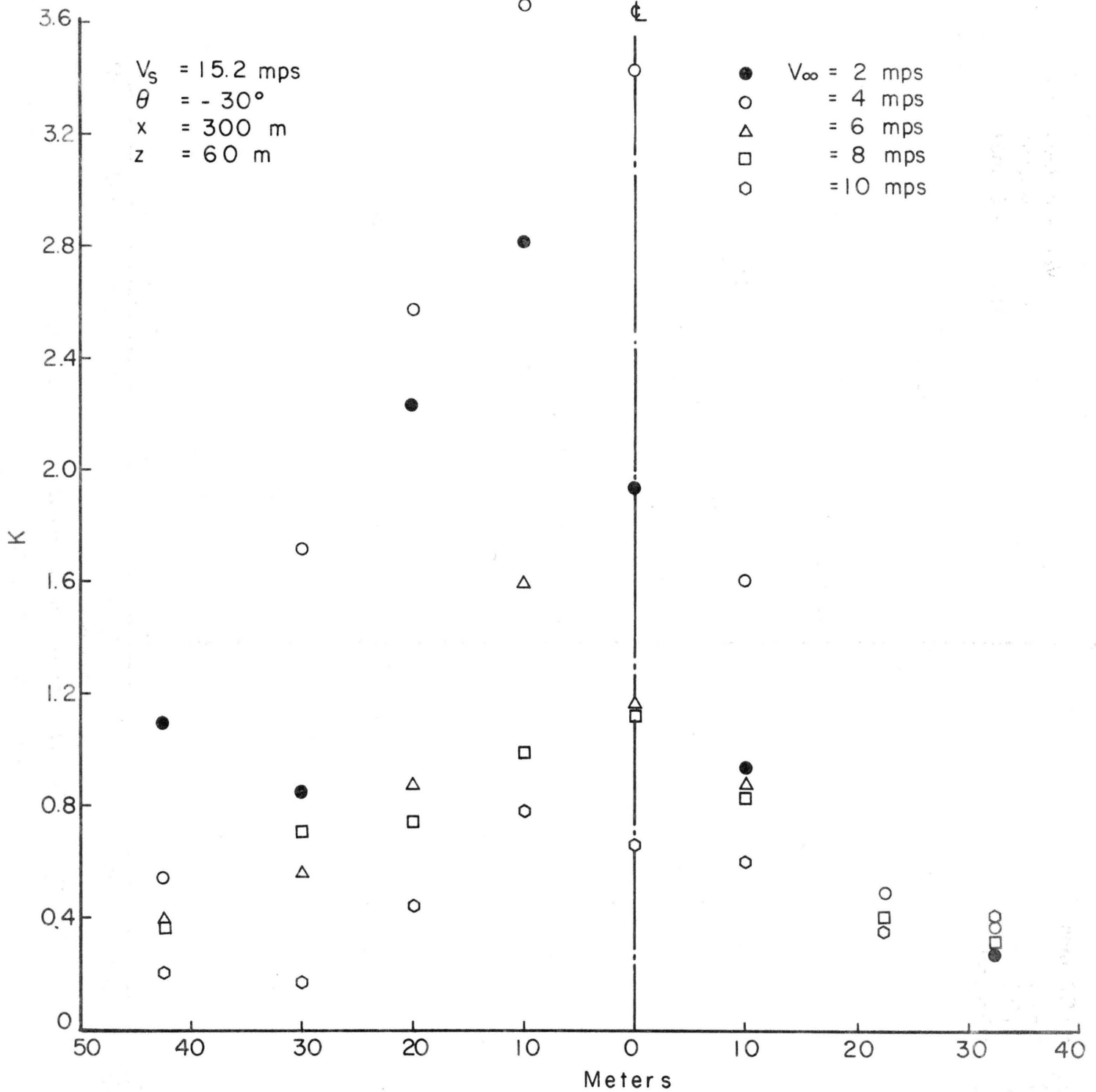
Fig. 16d. K-Profile for Gas Released at V_s = 15.2 mps,
θ = 330° , $\mathring{Q}$ = 425.0 m^3/min
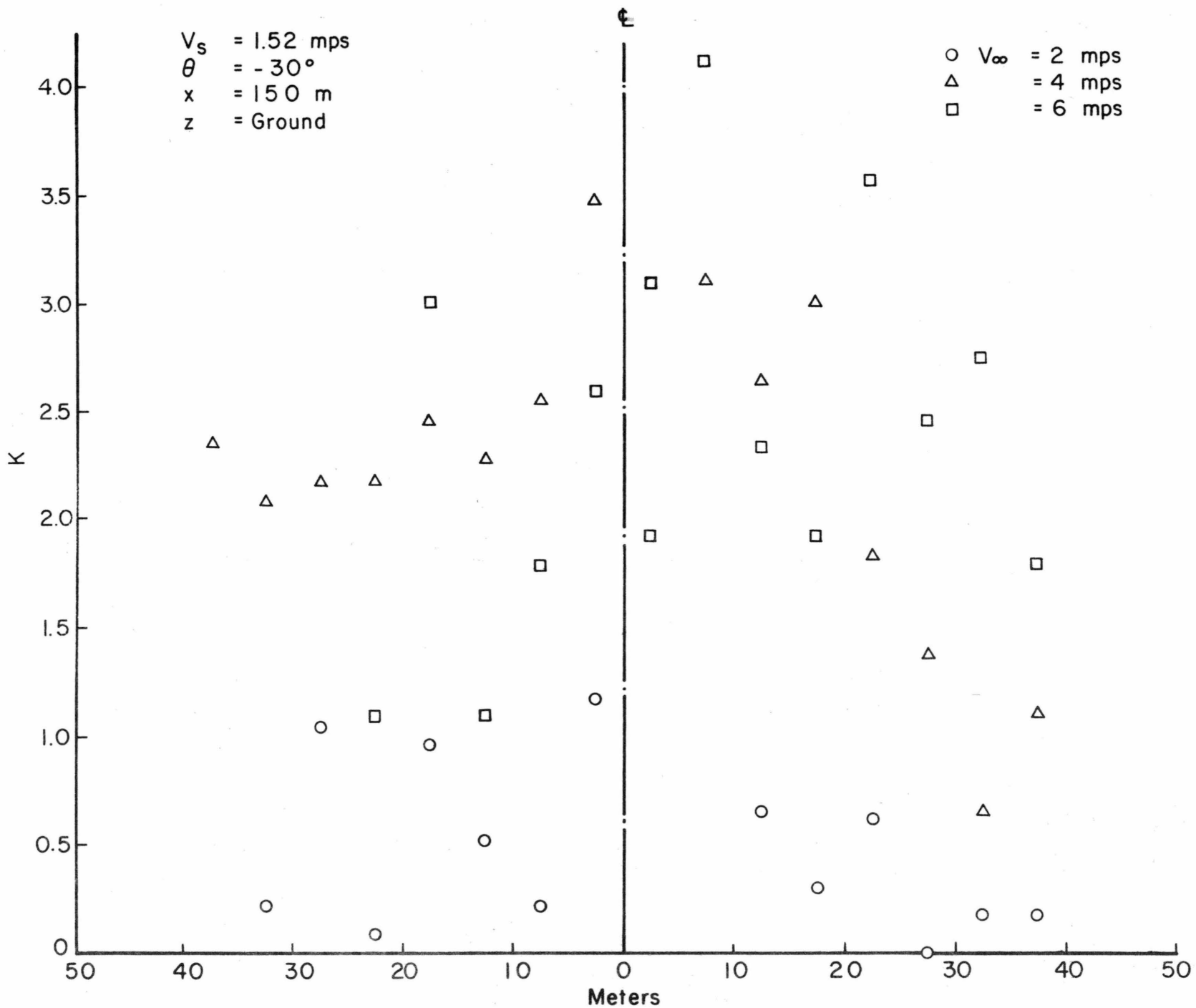
Fig. 17a. K-Profile for Gas Released at V_s = 15.8 mps, θ = 330° , $\mathring{Q}$ = 28.3 m^3/min

Fig. 17b. K-Profile for Gas Released at V_s = 15.8 mps,
θ = 330°, $\mathring{Q}$ = 28.3 m³/min

$V_s = 15.2$ mps
$\theta = -30°$
$x = 150$ m
$z = 60$ m

○ $V_\infty = 2$ mps
△ $= 4$ mps
□ $= 6$ mps

K

Meters
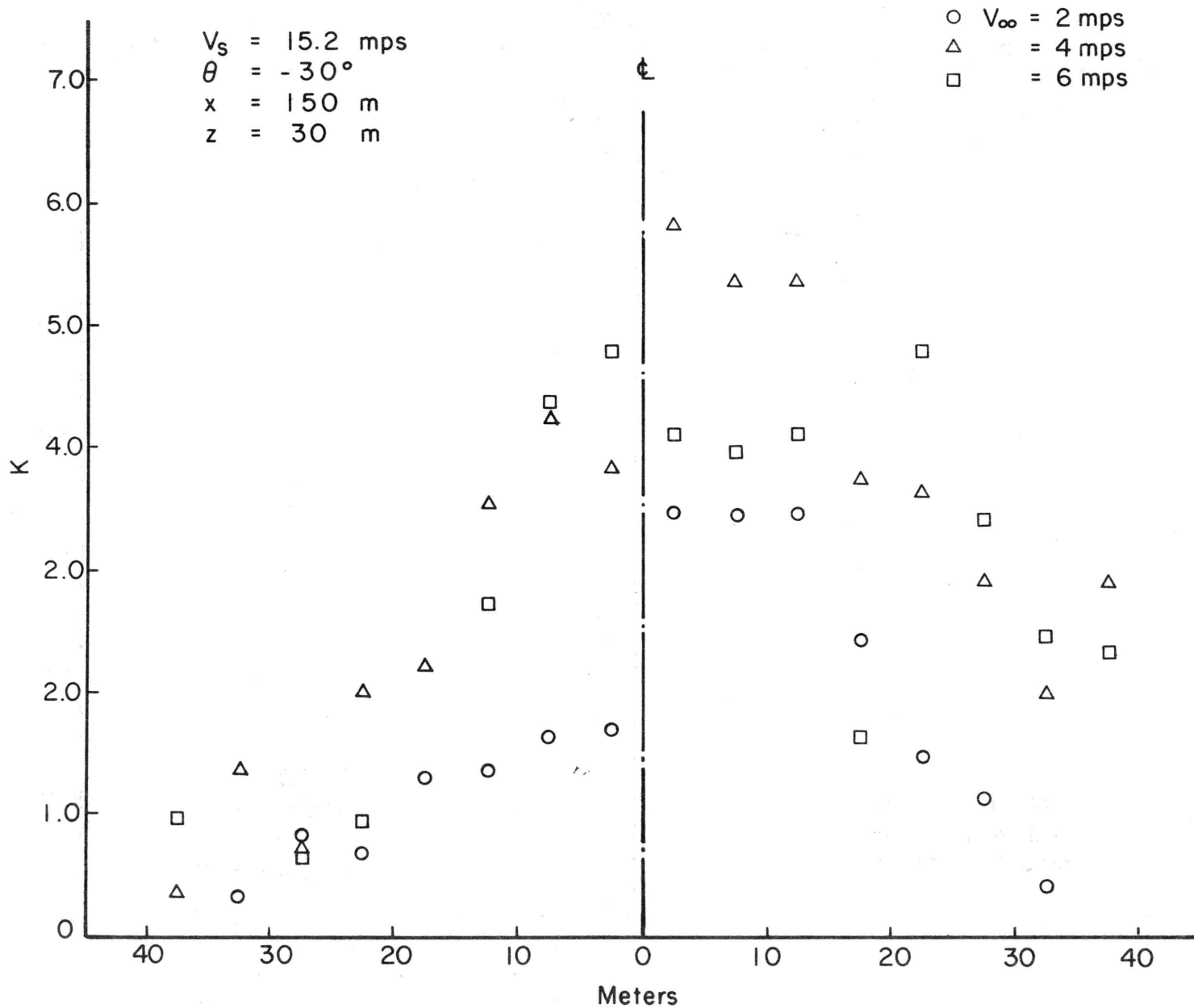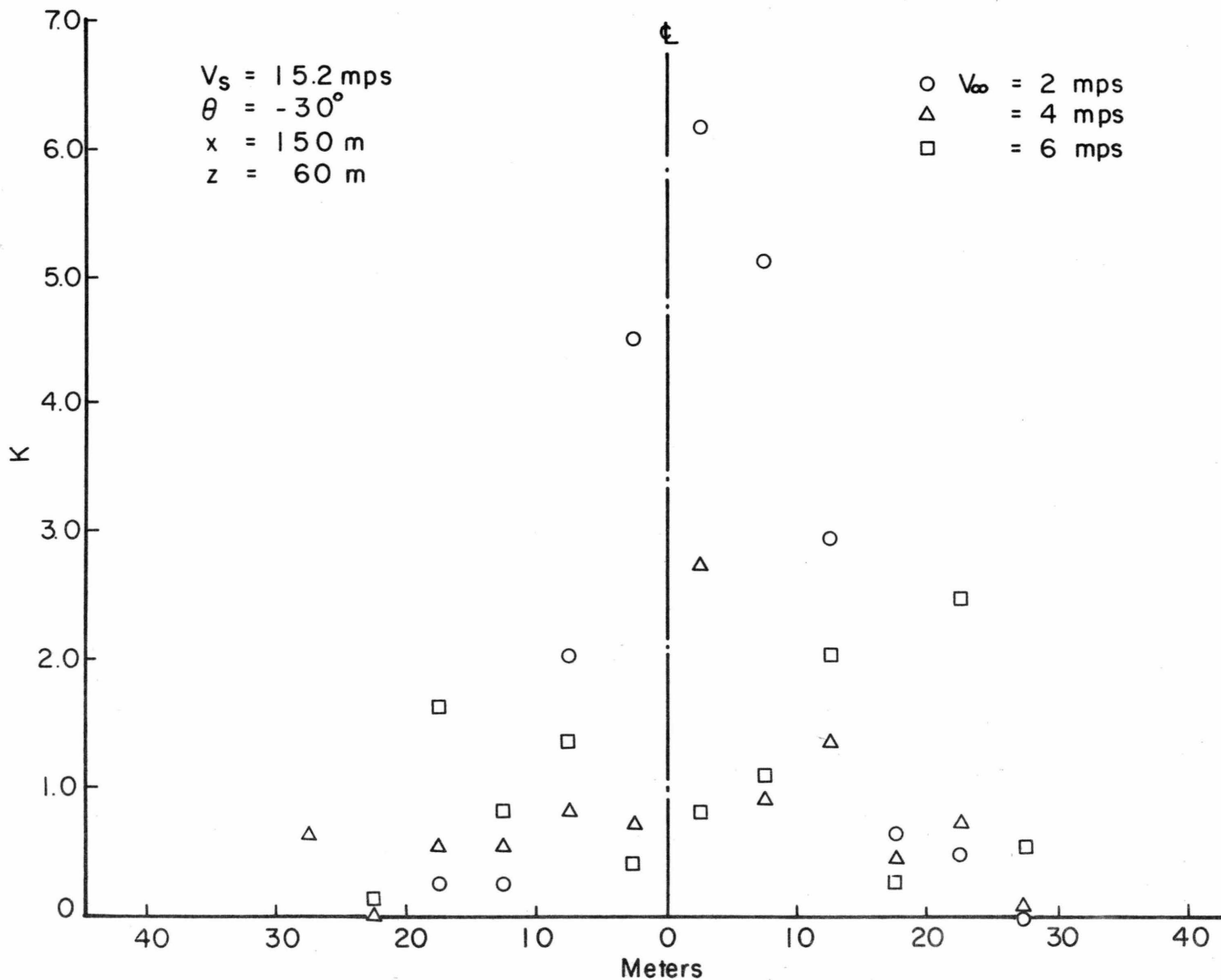
Fig. 17c. K-Profile for Gas Released at $V_s = 15.8$ mps,
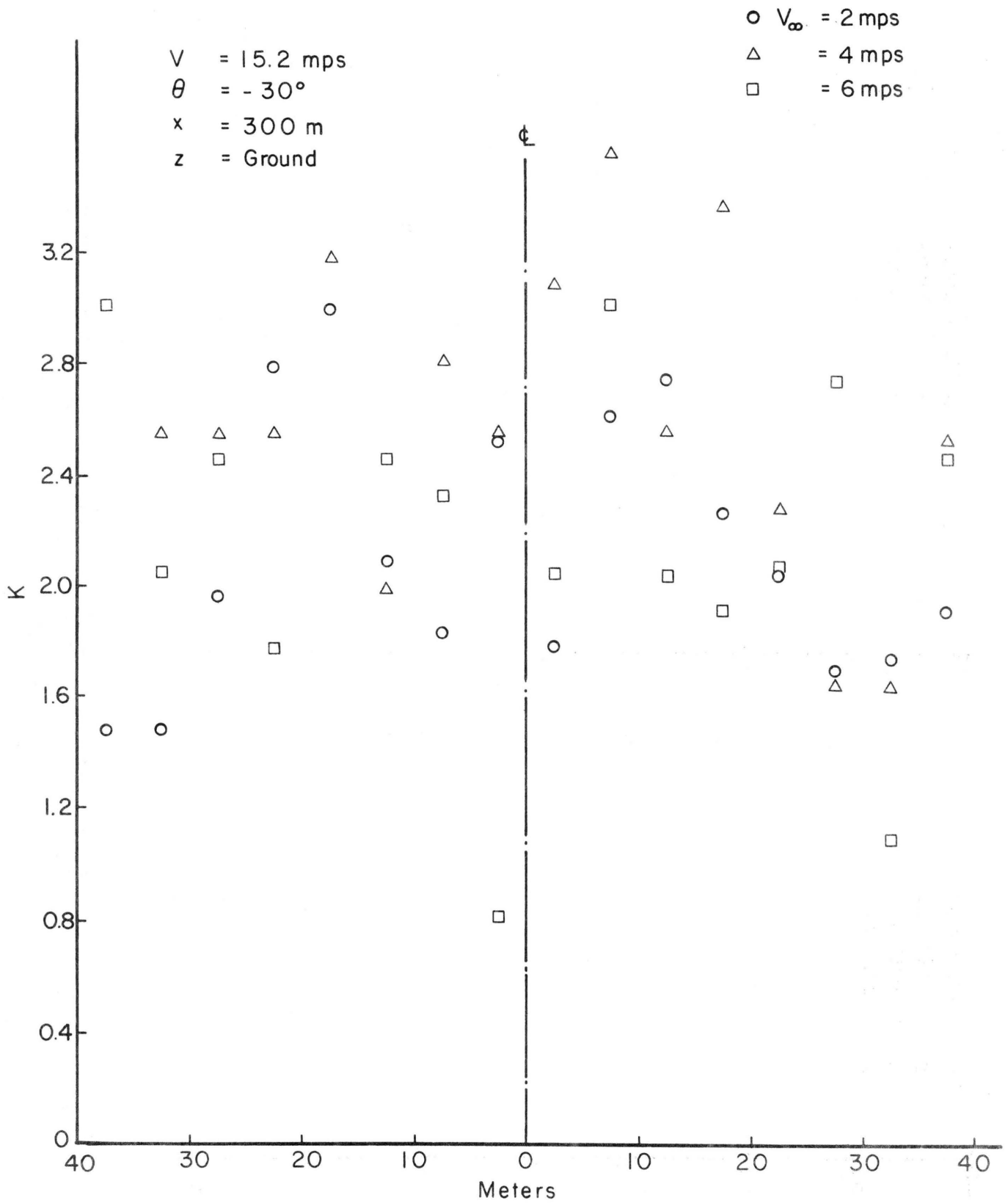
$\theta = 330°$, $\mathring{Q} = 28.3$ m^3/min

Fig. 17d. K-Profile for Gas Released at V_s = 15.8 mps,
θ = 330°, $\mathring{Q}$ = 28.3 m³/min
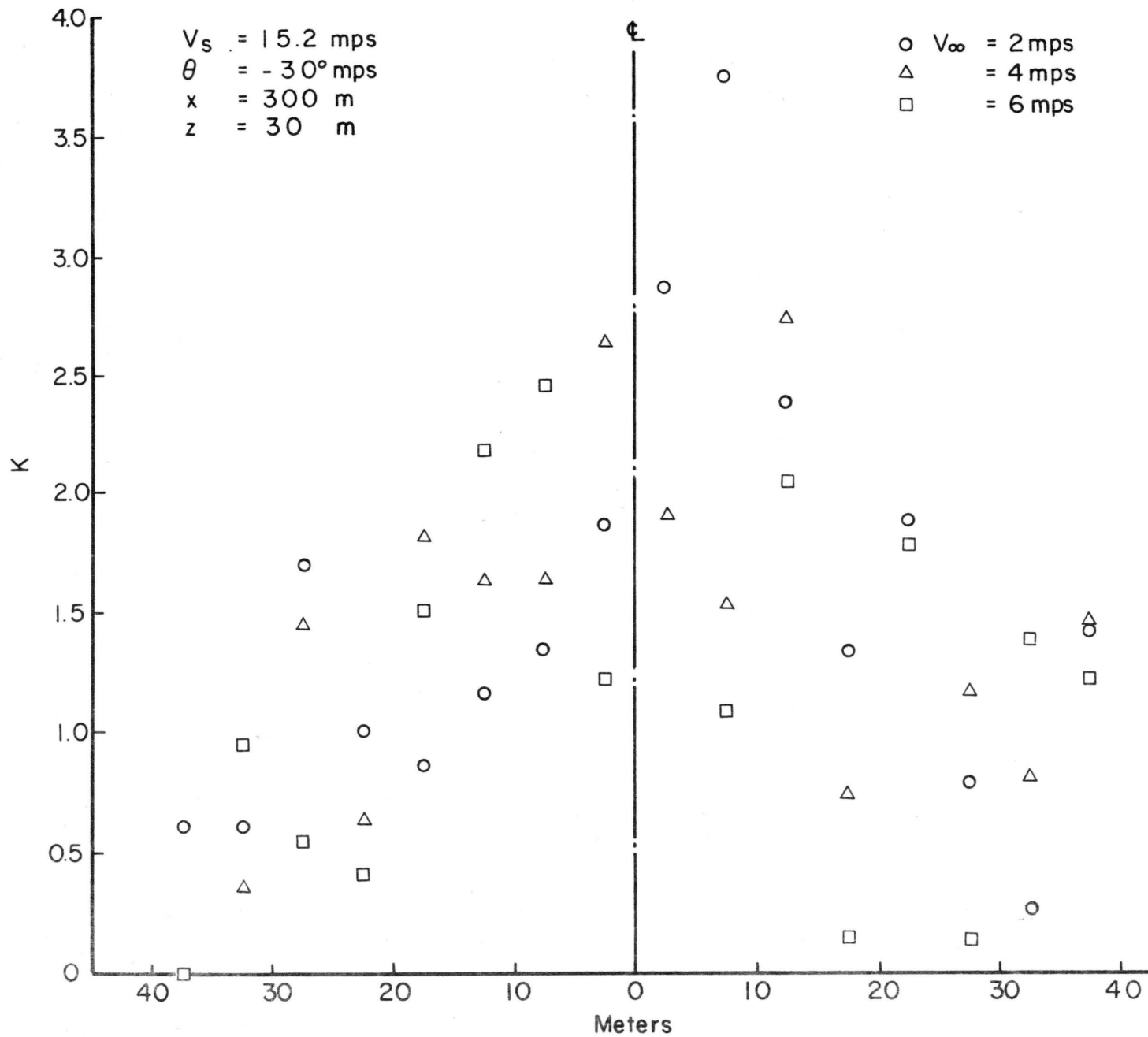
Fig. 17e. K-Profile for Gas Released at $V_s = 15.8$ mps,
$\theta = 330^\circ$, $\overset{\circ}{Q} = 28.3$ m³/min
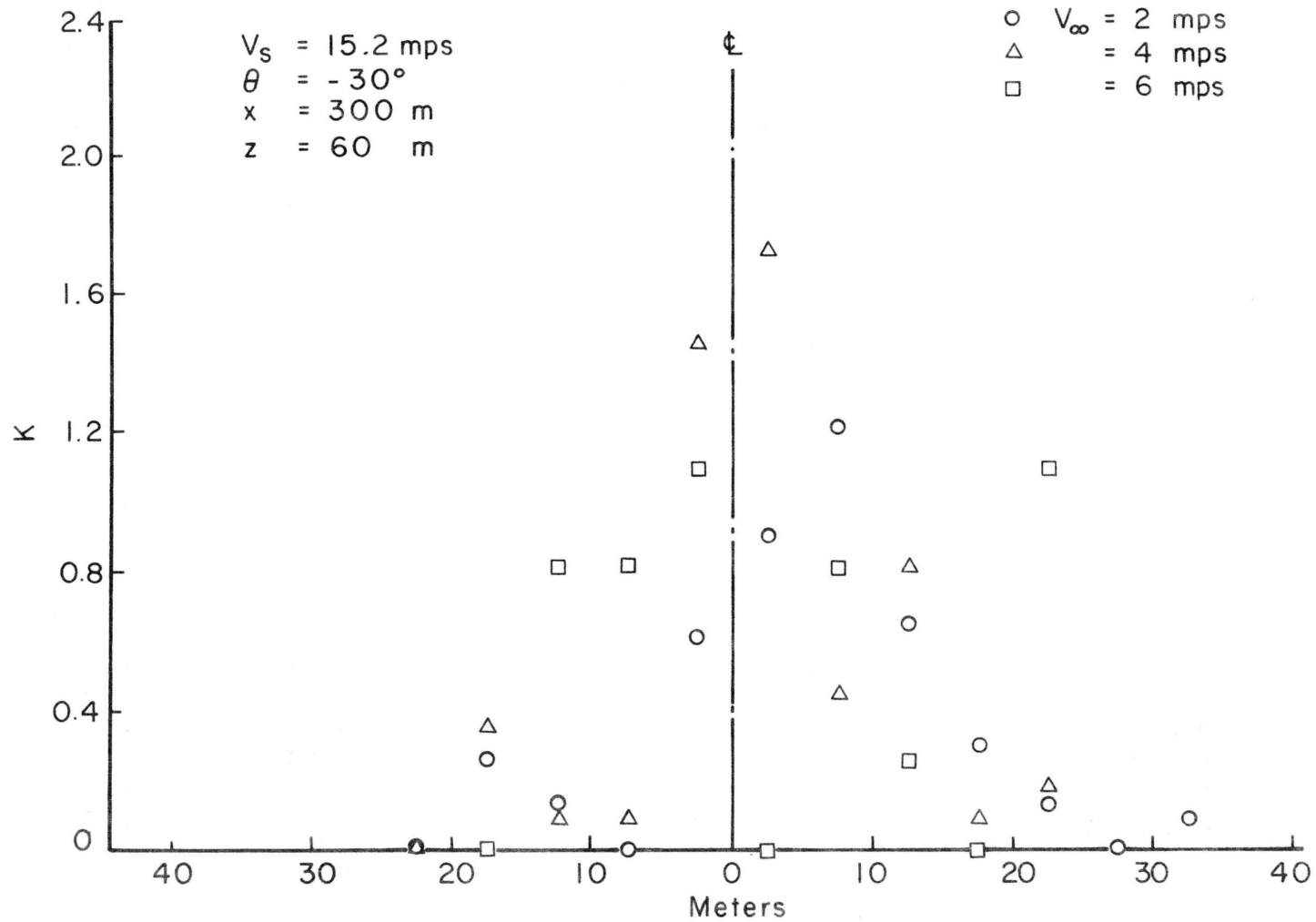
Fig. 17f. K-Profile for Gas Released at V_s = 15.8 mps,
θ = 330°, $\mathring{Q}$ = 28.3 m³/min
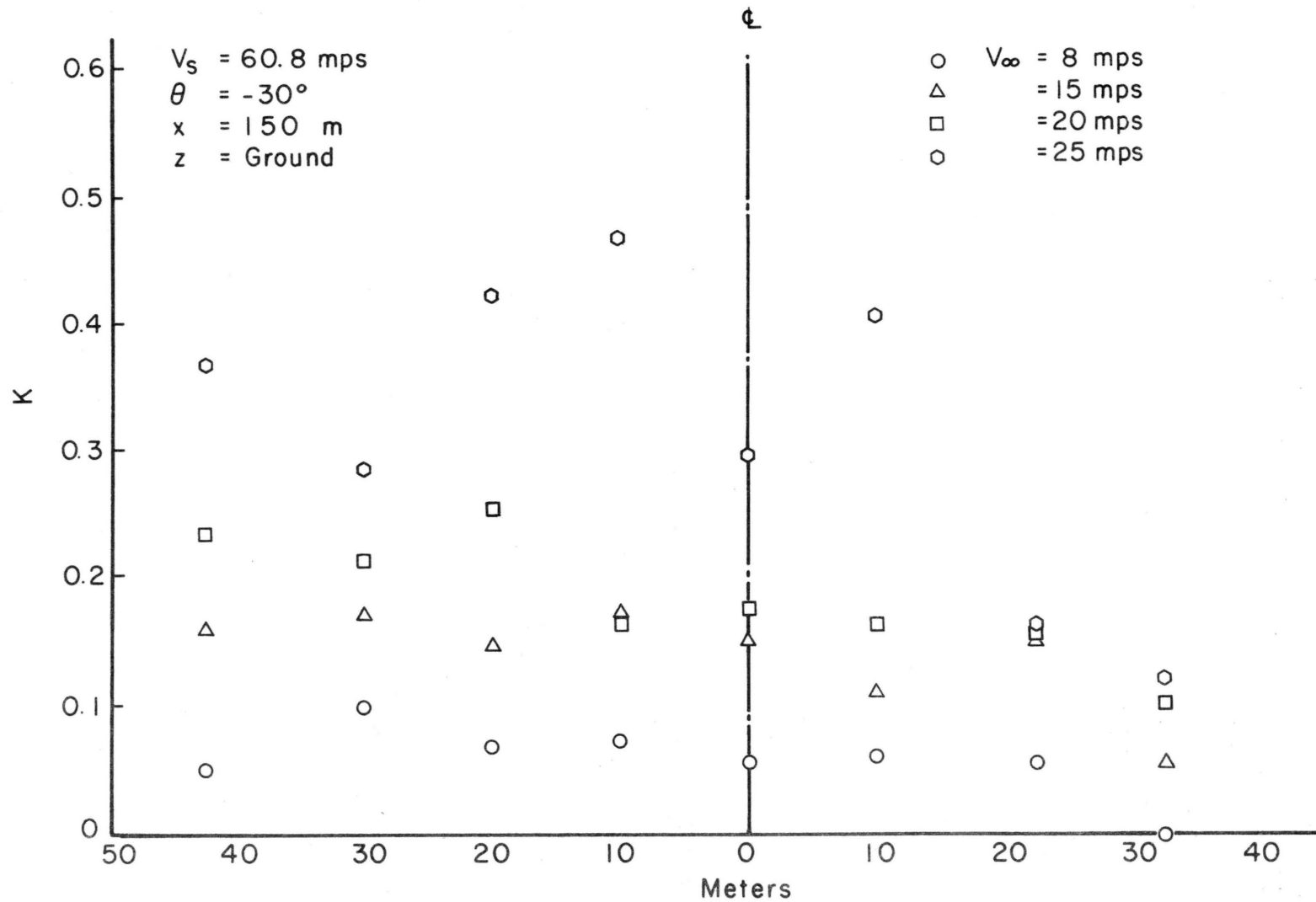
Fig. 18a. K-Profile for Gas Released at $V_s = 60.8$ mps, $\theta = 330^\circ$, $\mathring{Q} = 1700$ m³/min
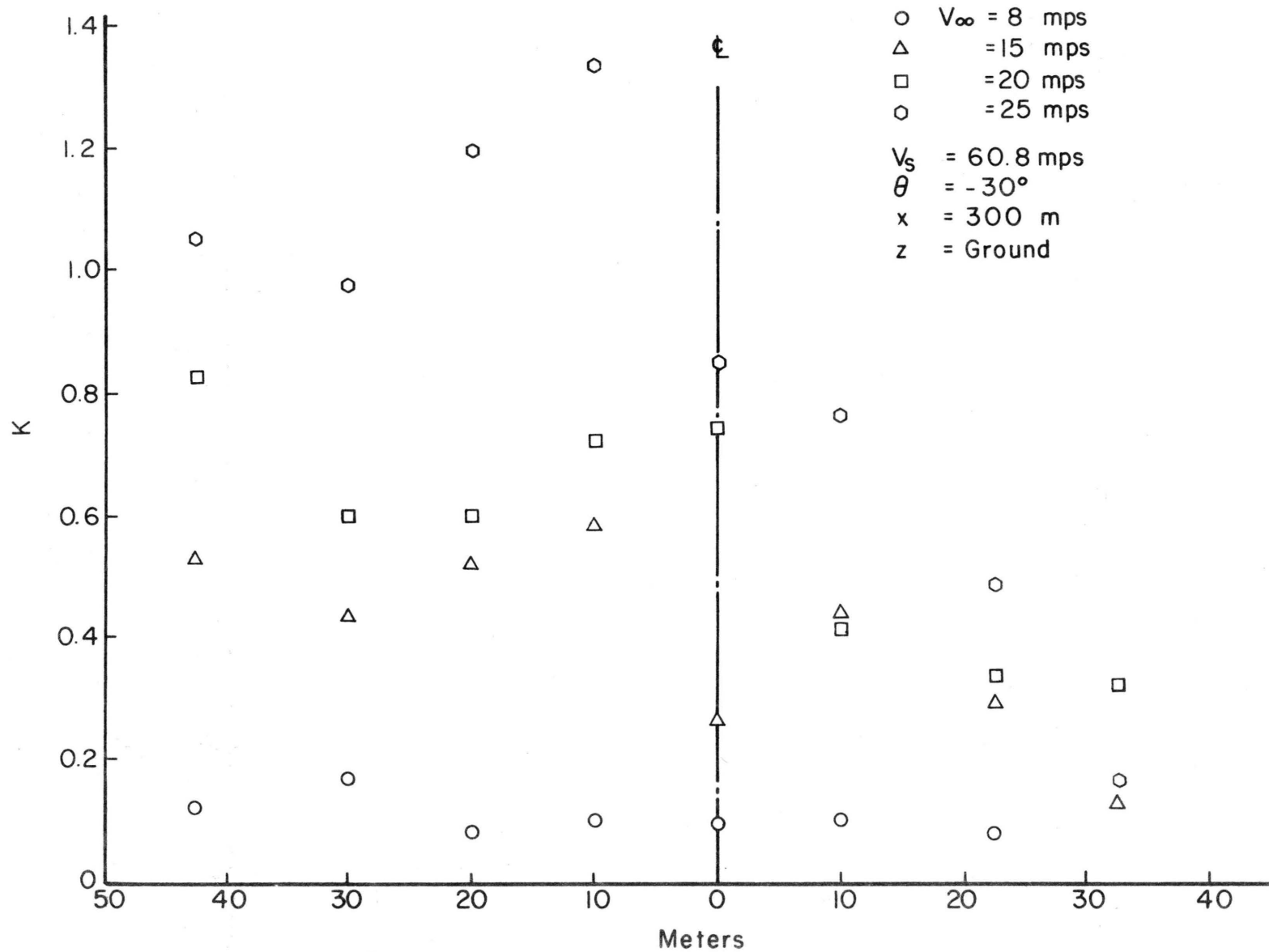
Fig. 18b. K-Profile for Gas Released at V_s = 60.8 mps,
θ = 330° , $\mathring{Q}$ = 1700 m³/min
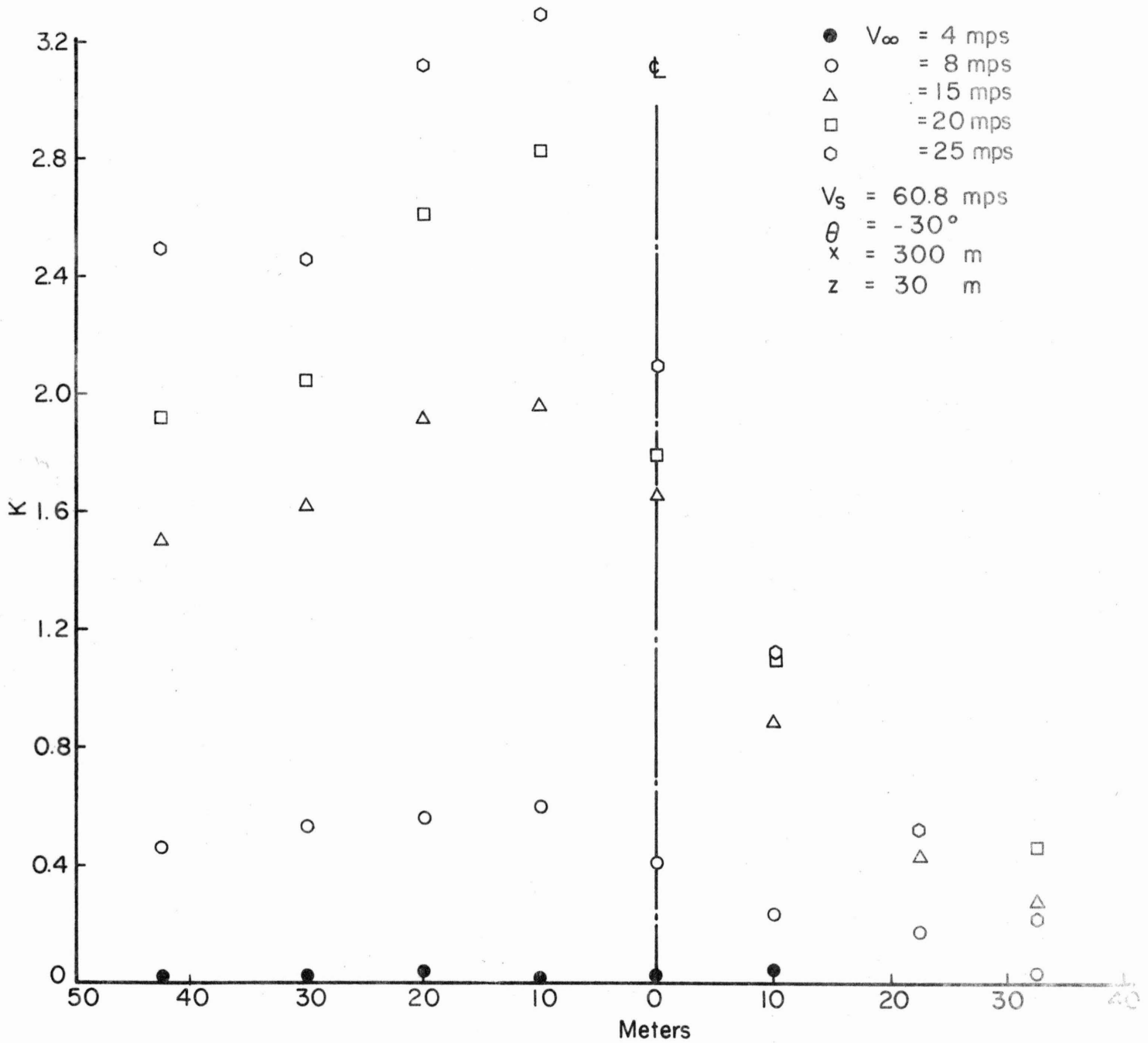
Fig. 18c. K-Profile for Gas Released at V_s = 60.8 mps, θ = 330°, $\mathring{Q}$ = 1700 m³/min
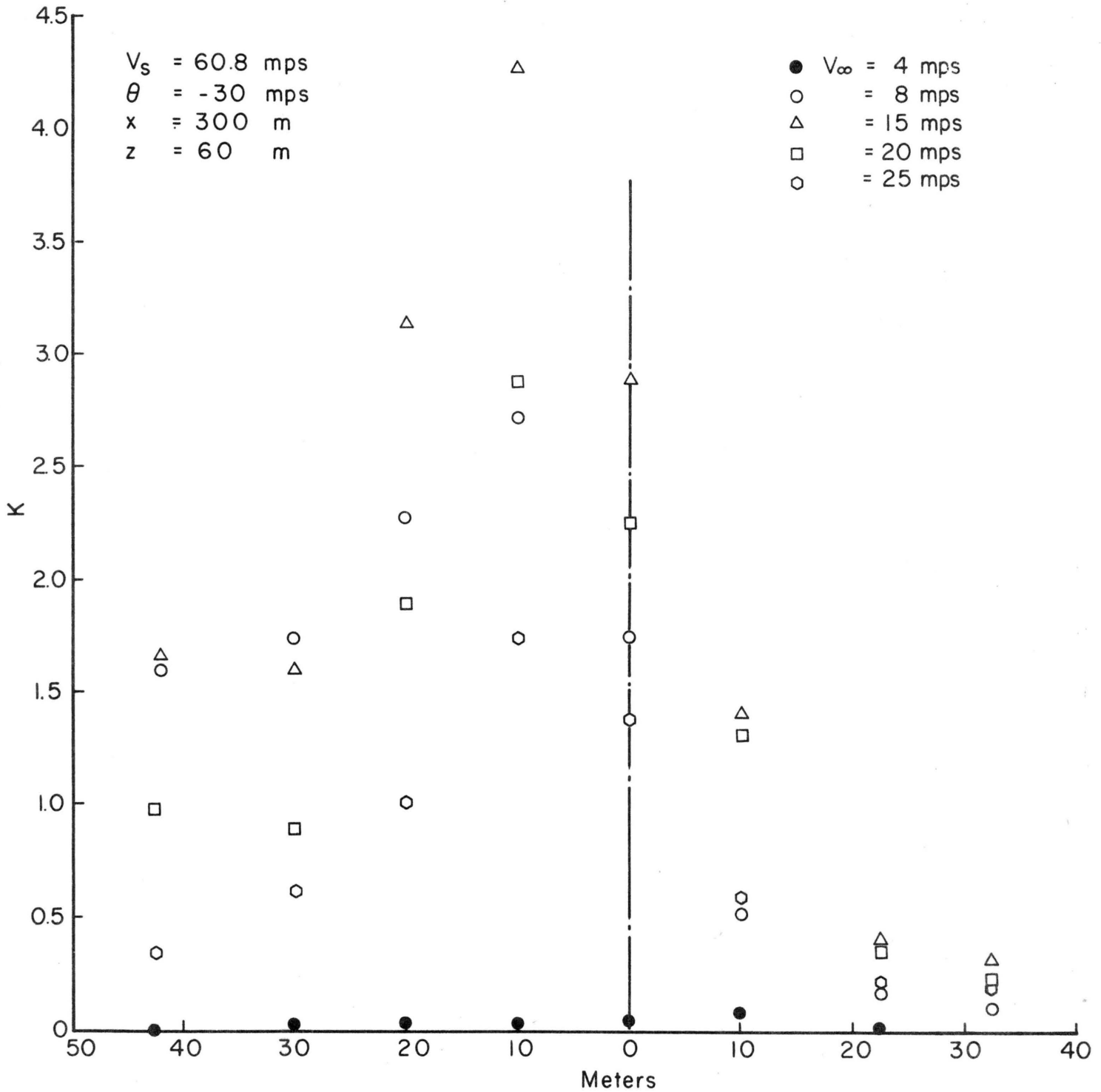
Fig. 18d. K-Profile for Gas Released at $V_s = 60.8$ mps, $\theta = 330^o$, $\mathring{Q} = 1700$ m^3/min

Fig. 19a. K-Profile for Gas Released at Various V_S/V_∞ Ratios
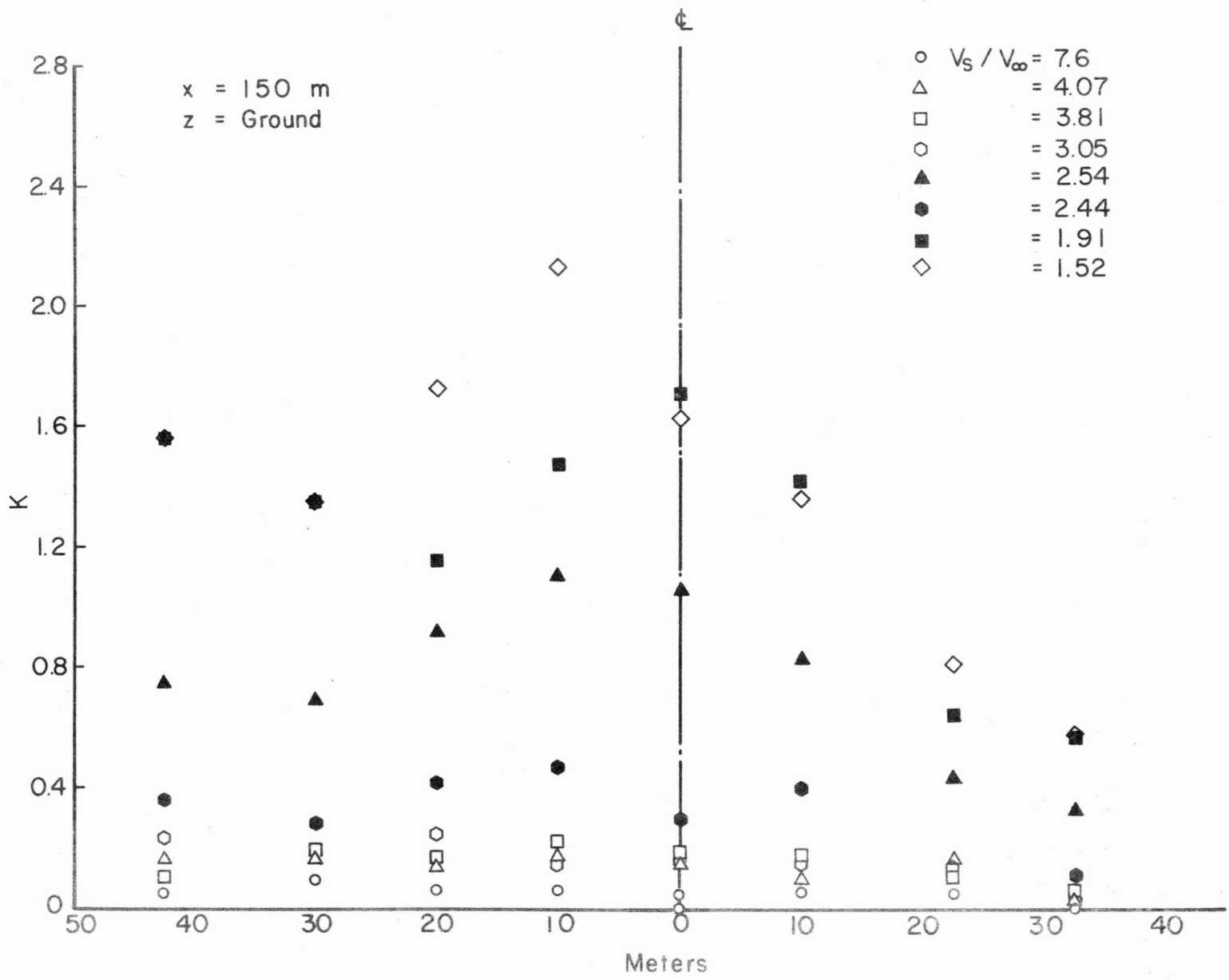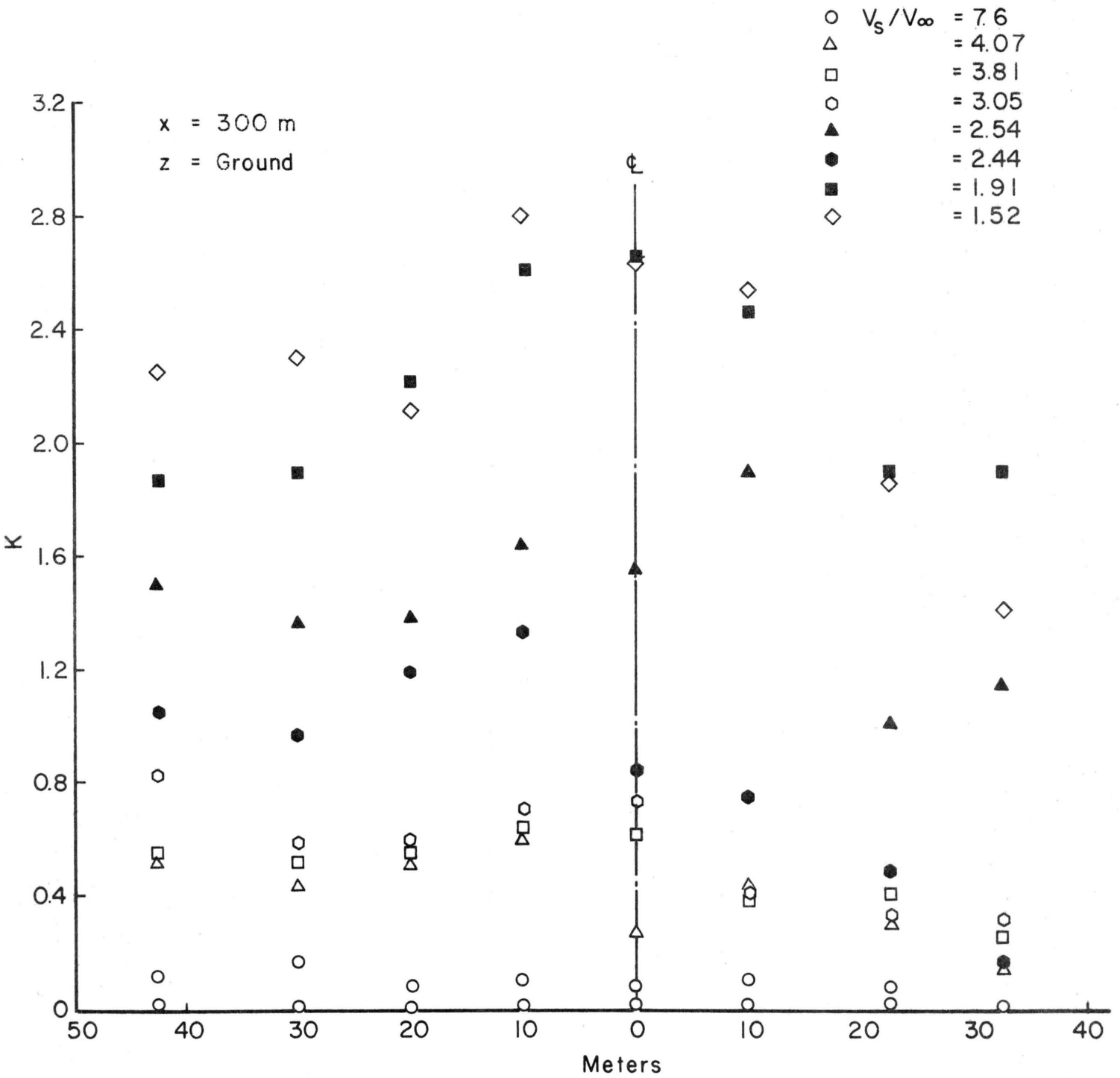
Fig. 19b. K-Profile for Gas Released at Various V_s/V_∞ Ratios
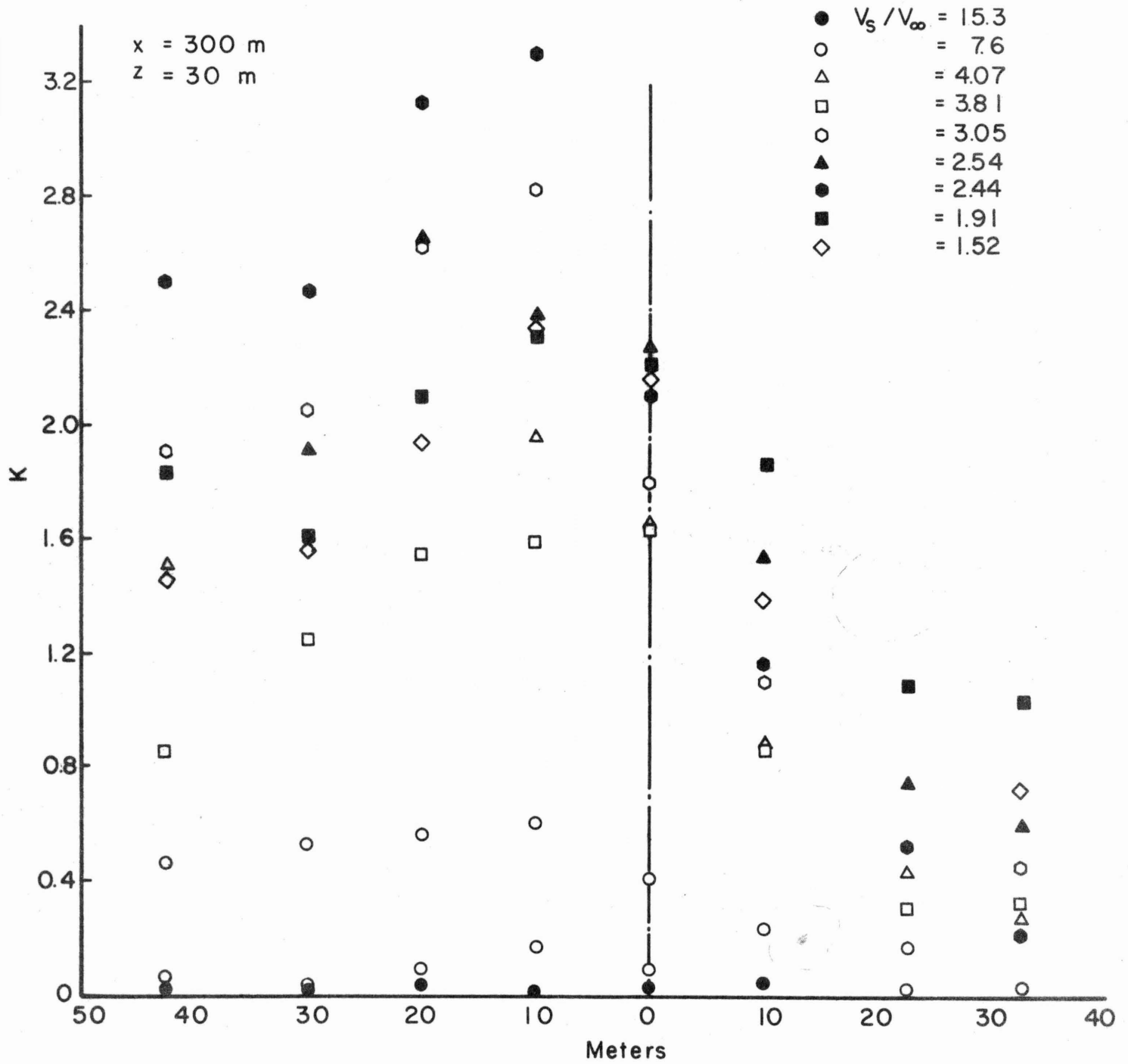
Fig. 19c.   K-Profile for Gas Released at Various V_S/V_∞ Ratios
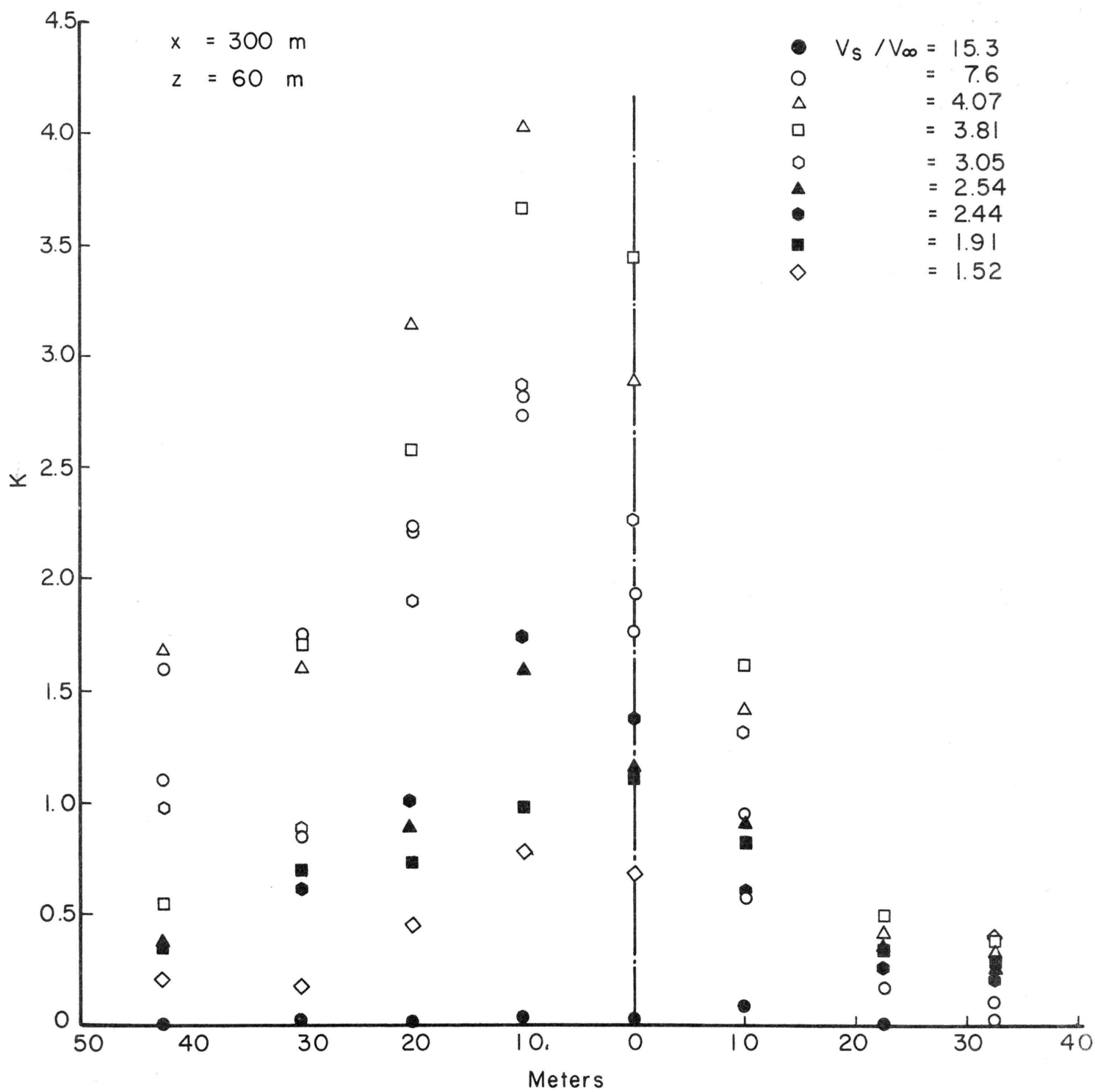
Fig. 19d. K-Profile for Gas Released at Various V_S/V_∞ Ratios
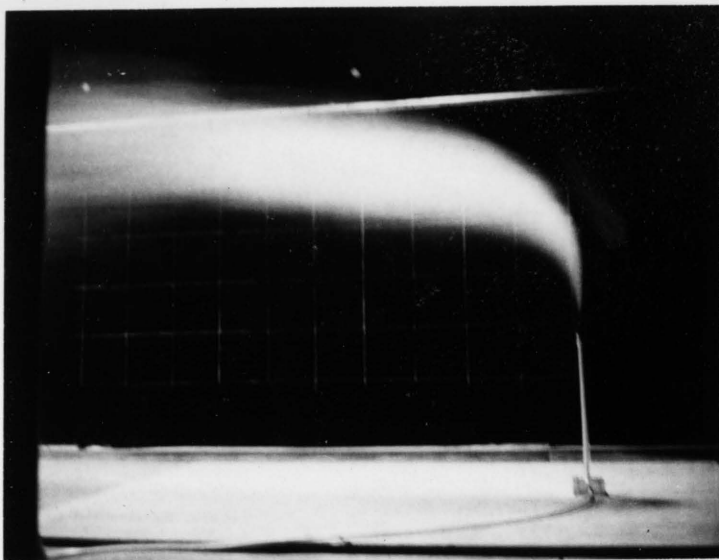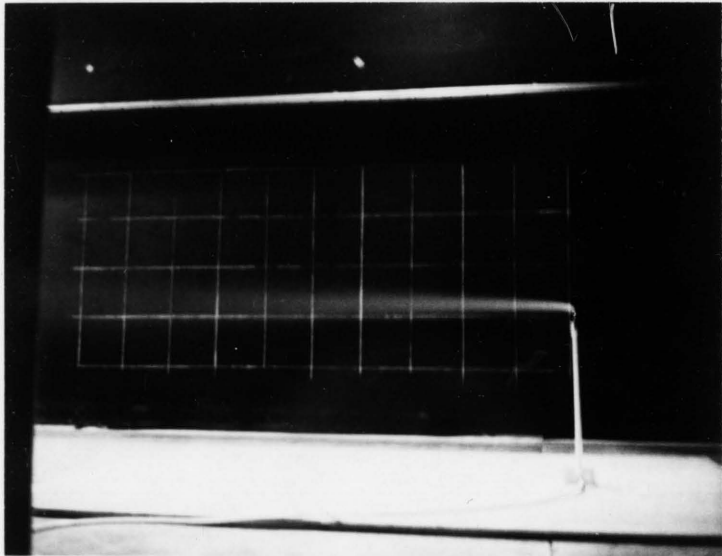
U∞ = 1 m/sec
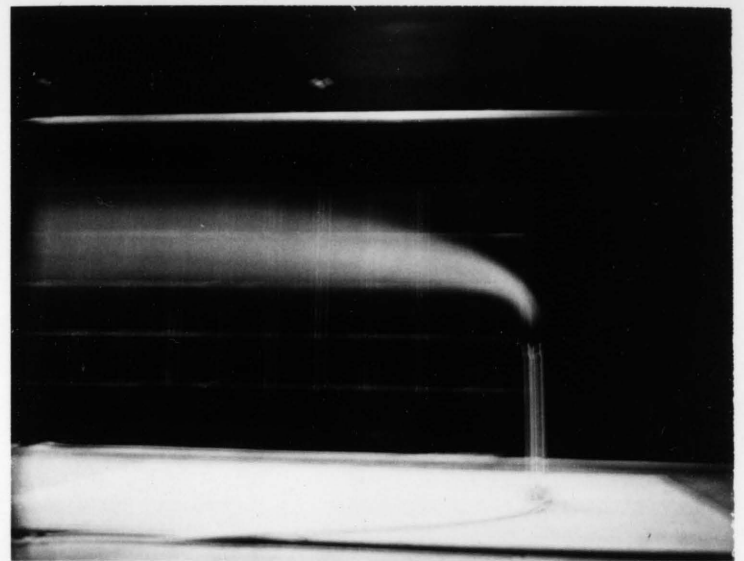
U∞ = 2 m/sec
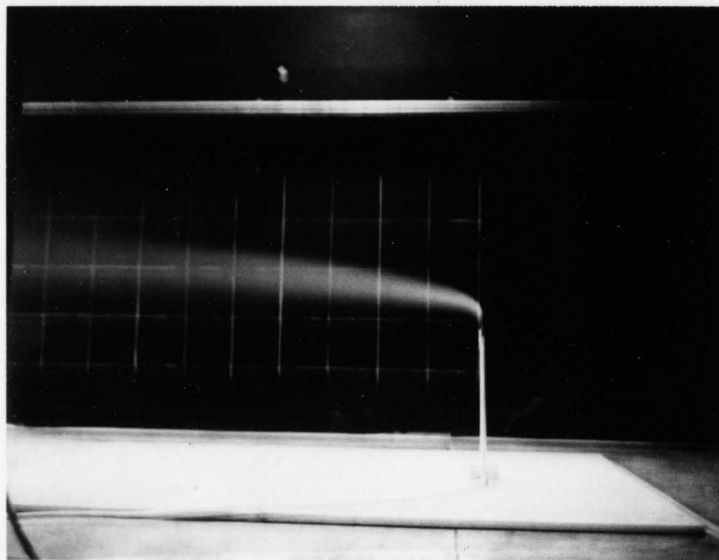
U∞ = 4 m/sec
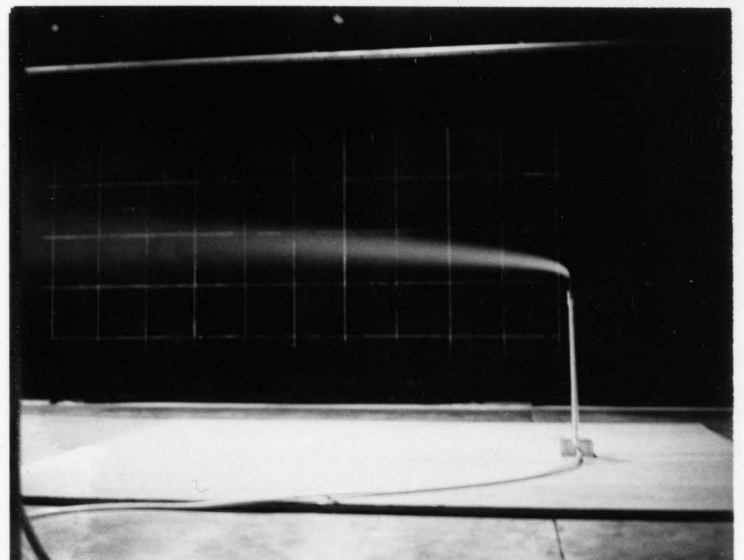
V = 15.2 m/sec

U∞ = 6 m/sec

Fig. 20a Smoke Plume for Simple Stack
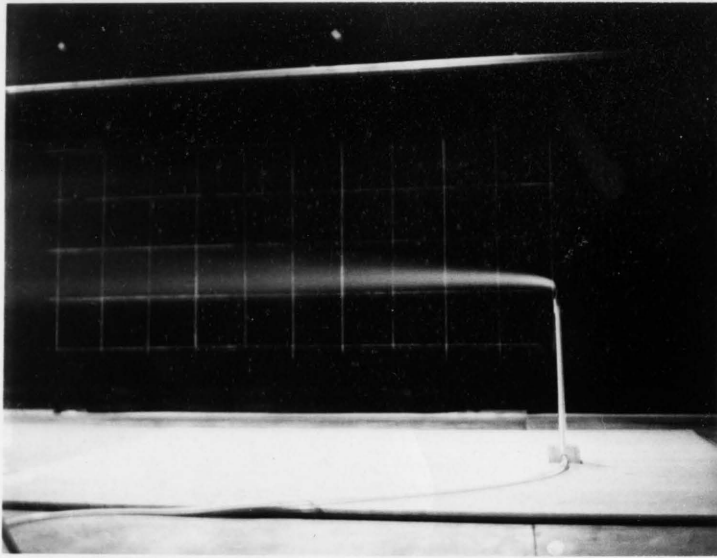
U_∞ = 8 m/sec
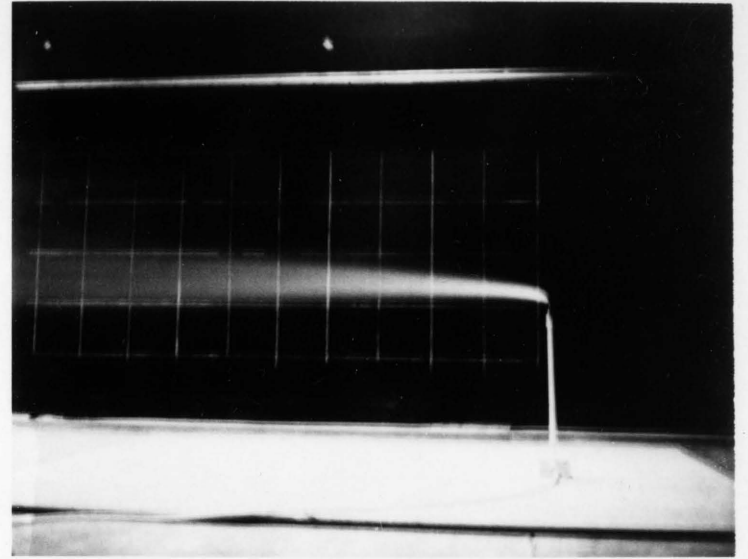
U_∞ = 10 m/sec

U_∞ = 15 m/sec
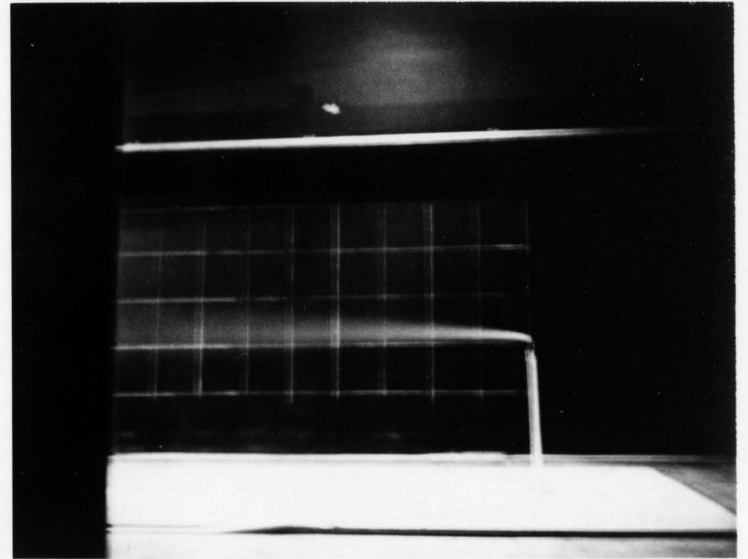
U_∞ = 20 m/sec

V_S = 15.2 m/sec

Fig. 20b Smoke Plume for Simple Stack